DETERMINATION OF THE HORIZONTAL DIFFUSION COEFFICIENT FOR USE IN THE SARMAP AIR QUALITY MODEL

FINAL REPORT
CONTRACT NO. 96-314

PREPARED FOR:

CALIFORNIA AIR RESOURCES BOARD
RESEARCH DIVISION
1001 I STREET
SACRAMENTO, CA 95814

PREPARED BY:

ROBERT J. YAMARTINO
MARK E. FERNAU

EARTH TECH, INC.
196 BAKER AVENUE
CONCORD, MA 01742

AND

SAVITHRI MACHIRAJU
MACHIRAJU AND ASSOCIATES

MAY 2000

For more information about the ARB's, Research Division's research and activities, please visit our Website:

http://www.arb.ca.gov/research/research.htm

TABLE OF CONTENTS

LIST OF FIGURES

LIST OF FIGURES (Continued)

LIST OF TABLES

ACKNOWLEDGMENTS

We thank Dr. Saffet Tanrikulu for providing SAQM codes and data and for being available to answer numerous questions about the SARMAP modeling system and Dr. Talat Odman for providing many insights into the results of the predecessor ARB project which implemented the alternative advection solvers into SAQM. We further acknowledge Drs. Odman and Tanrikulu for their insightful comments on the draft final report. We also thank Drs. Nehzat Motallebi and Bart Croes for providing technical and administrative guidance during the project. Finally, we thank Ms. Rebecca Arsenault for her technical editing of the manuscript.

This report was submitted in fulfillment of ARB Contract Number 96-314 entitled "Determination of the Horizontal Diffusion Coefficient for Use in the SARMAP Air Quality Model," by Earth Tech, Inc. Work was completed as of February 29, 2000.

ABSTRACT

The California Air Resources Board (ARB) Request for Proposals (RFP), entitled "Determination of the Horizontal Diffusion Coefficient for Use in Air Quality Models," identified three advection solvers that are already available for use within the SARMAP Air Quality Model (SAQM) and called for the theoretical formulation, experimental quantification, and within-SAQM sensitivity testing of diffusivity formulations that will yield net levels of pollutant dispersion that accurately mimic reality. Such a diffusivity formulation must account for the dominant atmospheric advective (e.g., wind shear) and turbulent transfer processes, compensate for smoothing or filtering present in the modeled wind fields, and correct for the unintended mixing processes accompanying present-day numerical advection schemes.

This study revealed that:

- the gridded MM-5 wind fields do cause some spatial smoothing of surface wind gradients, but retain 50-80% of the observed gradients, and are therefore quite useful for correcting the pollutant transport scheme for wind-/concentration-gradient effects;

- such wind gradient-related transport terms yield small changes in surface ozone concentrations;

- as the MM-5 wind fields already include most wind directional shear with height, an important mechanism in lateral dispersion, avoidance of "double-counting" of such shear influences demands that explicitly-modeled dispersion rates and diffusivities exclude such shear influences -- a fact which greatly reduces the usefulness of most tracer experiment results, as real-world experiments include all mechanisms;

- a numerical simulation using the synthetic turbulence model, KSP, suggested that an appropriate lateral diffusivity for 10km wide plumes in an atmosphere free of directional shear is of order $u^* \cdot \sigma_y$, where u^* is the friction velocity and σ_y is the plume's lateral standard deviation;

- extension of this concept throughout the PBL leads to a physical, non-dimensional diffusivity of $k_H = 0.2 \cdot i_y \cdot \varepsilon$, where i_y is the local turbulent intensity, σ_v/U, and ε is the local Courant number, $U \cdot \Delta t / \Delta x$;

- the long-wave numerical diffusivities of the Bott (BOT) and Yamartino (YAM) advection schemes are comparable, larger than those of the Accurate Space Derivative (ASD) scheme, and are modeled in terms of the local Courant number, ε, and the fourth-derivative of the local concentration distribution;

- the short-wave (i.e., $\lambda/\Delta x = 2$ and 3) performance of the three advection schemes differs markedly, includes some non-diffusive and/or non-linear effects (e.g., anti-diffusion, hole-burning), and is not presently modeled as a diffusivity; and,

- SAQM peak daily ozone decreases 10-15 ppb when a plausible level of lateral diffusion is included, and the numerical-diffusion-corrected predictions of the three transport schemes generally agree to within a few ppb, though some differences are as large as 10%.

EXECUTIVE SUMMARY

The California ARB's RFP, "Determination of the Horizontal Diffusion Coefficient for Use in Air Quality Models," identified three advection solvers that are already available for use within the SARMAP Air Quality Model (SAQM) and called for the theoretical formulation, experimental quantification, and within-SAQM sensitivity testing of diffusivity formulations that will yield net levels of pollutant dispersion that accurately mimic reality. Such a diffusivity formulation must account for the dominant atmospheric advective (e.g., wind shear) and turbulent transfer processes, compensate for smoothing or filtering present in the modeled wind fields, and correct for the unintended mixing processes accompanying present-day numerical advection schemes.

A number of issues and phenomena were examined in detail as part of this study. First, the magnitude and constituent components of lateral diffusion in the atmosphere were reviewed. Given the very significant role of wind shear (e.g., shears at a particular horizontal level and turning of the wind direction with height) in the lateral diffusion process, MM-5's ability to capture wind shears was examined. Despite its similarly coarse horizontal spatial resolution, MM-5 captures 50-80% of the shear measured over separations greater than three grid cells. This suggests that the shear correction module developed for SAQM as part of this study can reasonably utilize the available MM-5 winds and achieve the appropriate advective redistribution of pollutants. MM-5's significantly higher vertical resolution assures it of capturing the important vertical wind shears, which in turn demands that the diffusivities that one utilizes in a SAQM lateral diffusivity module not "double count" this important effect. As a result, a more appropriate horizontal diffusion coefficient has been computed with the aid of a synthetic turbulence model, KSP, that can simulate lateral dispersion in an artificial atmosphere that is free of such vertical wind shear. KSP results indicated that an appropriate lateral diffusivity for 10km wide plumes in a neutral atmosphere, free of directional shear, is of order $u^* \cdot \sigma_y$, where u^* is the friction velocity and σ_y is the plume's lateral standard deviation. Extension of this concept throughout the PBL then led to a physical, non-dimensional diffusivity of $k_H = 0.2 \cdot i_y \cdot \varepsilon$, where i_y is the local turbulent intensity, σ_v/U, and ε is the local Courant number, $U \cdot \Delta t / \Delta x$. The resulting diffusivity module thus utilizes micrometeorologically-based estimates of the standard deviation of lateral velocity, σ_v, times a constant and the grid resolution, Δx, of the modeling domain.

The resulting SAQM lateral diffusivity module also incorporates the results of our investigation and subsequent parameterization of numerical diffusion. This aspect of the study revealed that the long-wave numerical diffusivities of the Bott (BOT) and Yamartino (YAM) advection schemes are comparable, larger than those of the Accurate Space Derivative (ASD) scheme, and are reasonably modeled in terms of the local Courant number, ε, and the fourth-derivative of the local concentration distribution. Numerical diffusion corrections for the Bott and Yamartino advection schemes were then implemented into the module code. The completed set of lateral transport and diffusivity modules was then smoothly and seamlessly integrated into the SAQM model simply via substitution of a number of SAQM's subroutines, and no changes to SAQM's preprocessor, input data formats, or control files were required.

Various versions of SAQM were then exercised on the August 3-6 SJVAQS ozone episode to evaluate the sensitivity of SAQM to the various components added during this study and compare the results using the three different advection schemes. These runs demonstrate that the SAQM

code modifications, designed to make the treatment of diffusion in SAQM more physically realistic, were properly integrated into the current operational version of the modeling system. In addition, the resulting ozone concentrations show that improving the physical basis of the SAQM code results in a more robust simulation, that is reduced sensitivity to the advection scheme used, and has a significant effect in reducing the size and location of ozone daily maxima. SAQM peak daily ozone decreases 10-15 ppb when a plausible level of lateral diffusion is included, and the numerical-diffusion-corrected predictions of the three transport schemes generally agree to within a few ppb, though some differences can be as large as 10%.

Persisting differences between the ASD results and those of Bott and Yamartino suggest that the relatively high, short-wave, numerical diffusivities in ASD must also be compensated for before the SAQM results can be said to be truly advection scheme independent. This may be possible within the existing framework via selection of a function that declines more rapidly with increasing wavelength. Should such a simple adjustment not suffice, in-depth investigations of the emissions field relative to the concentration differences and trajectory studies may be needed to reveal more information about any transport-related aspects of the concentration differences.

Thus, in summary, this study revealed that:

- the gridded MM-5 wind fields do cause some spatial smoothing of surface wind gradients, but retain 50-80% of the observed gradients, and are therefore quite useful for correcting the pollutant transport scheme for wind-/concentration-gradient effects;

- such wind gradient-related transport terms yield small changes in surface ozone concentrations;

- as the MM-5 wind fields already include most wind directional shear with height, an important mechanism in lateral dispersion, avoidance of "double-counting" of such shear influences demands that explicitly-modeled dispersion rates and diffusivities exclude such shear influences -- a fact which greatly reduces the usefulness of most tracer experiment results, as real-world experiments include all mechanisms;

- a numerical simulation using the synthetic turbulence model, KSP, suggested that an appropriate lateral diffusivity for 10km wide plumes in an atmosphere free of directional shear is of order $u^* \cdot \sigma_y$, where u^* is the friction velocity and σ_y is the plume's lateral standard deviation;

- extension of this concept throughout the PBL leads to a physical, non-dimensional diffusivity of $k_H = 0.2 \cdot i_y \cdot \varepsilon$, where i_y is the local turbulent intensity, σ_v/U, and ε is the local Courant number, $U \cdot \Delta t / \Delta x$;

- the long-wave numerical diffusivities of the Bott (BOT) and Yamartino (YAM) advection schemes are comparable, larger than those of the Accurate Space Derivative (ASD) scheme, and are modeled in terms of the local Courant number, ε, and the fourth-derivative of the local concentration distribution;

- the short-wave (i.e., $\lambda/\Delta x = 2$ and 3) performance of the three advection schemes differs markedly, includes some non-diffusive and/or non-linear effects (e.g., anti-diffusion, hole-burning), and is not presently modeled as a diffusivity; and,

- SAQM peak daily ozone decreases 10-15 ppb when a plausible level of lateral diffusion is included, and the numerical-diffusion-corrected predictions of the three transport schemes generally agree to within a few ppb, though some differences are as large as 10%.

Details of the study and the resulting SAQM code modifications are presented in this Final Report.

1. INTRODUCTION

The SARMAP Air Quality Model (SAQM) (Jin and Chang, 1993; Chang et al., 1993; Chang et al., 1996) was developed and evaluated for State Implementation Plan (SIP) development over the San Joaquin Valley, the second most problematic ozone domain in California (and the U.S.). Based on the RADM acid rain model of the 1980's, SAQM is a modern, high-resolution (i.e., 15-17 vertical layers) photochemical grid model, driven by the Penn State/NCAR prognostic, mesoscale meteorological model, MM-5 (Dudhia, 1993; Stauffer and Seaman, 1994; Seaman et al., 1995). Both models utilize a horizontal mesh resolution of 12-km over the entire Central Valley domain of interest, with 4-km resolution nesting possible over several major urban areas. The SARMAP modeling system (MM-5 plus SAQM and MM-5/SAQM interface programs) was evaluated using data obtained during the SJVAQS (i.e., the SARMAP field program) of August 1990 and, in particular, for the ozone episode days of August 3-6, 1990 (DaMassa et al., 1996). While the SARMAP modeling system satisfied stated ARB and EPA performance criteria (Tesche et al., 1990), various deficiencies have prompted various SAQM modifications. These modifications include increased vertical resolution near the surface, the addition of a reactive plume submodule, and the addition of two alternative advection algorithms (Tanrikulu and Odman, 1996) during an earlier ARB project (Odman et al., 1996). Finally, recognition of the crudeness with which horizontal diffusion is modeled in this, and most other, grid models, and the importance of this dispersion mechanism in determining concentrations of primary and secondary species, the present study was undertaken.

The Request for Proposals (RFP) defined two types of nonphysical horizontal diffusion relevant to the problem of determining the appropriate "actual" (or physically-based) horizontal diffusion coefficients, K_H, that should be used when simulating horizontal diffusion in a model. These are:

- "numerical" diffusion - resulting from "errors" in the advection scheme, and
- "artificial" diffusion - resulting from the instantaneous dilution of emissions and concentrations by the finite volume of the grid cells.

The basic goal of this study is to determine all the processes in the atmosphere that lead to the "total" horizontal diffusion or smearing of material in nature, and then represent the SAQM's "actual" horizontal diffusion coefficient as:

$$\text{actual} = \text{total} - (\text{numerical} + \text{artificial}). \quad (1)$$

The specified actual diffusion coefficient, when combined with the effects of the input wind fields, the numerical diffusion of the advection scheme, and the artificial diffusion associated with grid models, should then accurately simulate the total diffusion that is observed to occur in the atmosphere. To achieve this goal, one must also know how to model or quantify the "numerical" and "artificial" terms for each of the candidate advection schemes. It also is important to realize that the "total" involves processes, such as wind shears, that are genuinely transportive rather than diffusive. Lumping such shear effects into the "total" diffusivity has previously been (Smagorinsky, 1963) an expedient way to treat them, though there is no reason not to explicitly

model these as advective terms in order to realize the correct "total" redistribution of material.

In the sections that follow, the various terms contributing to Equation (1) will be discussed in detail. The report begins with an introduction to the subject of horizontal advection and diffusion in operator split photochemical models, an overview of the candidate advection schemes and their properties and constraints, and a discussion of the issues addressed during the project. Such issues include: numerical diffusion, the pros and cons of using diffusivities to represent advective processes (e.g., wind shears), turbulent diffusion, and operator splitting-induced errors and their correction. To the extent possible, the report is partitioned to correspond to the contractual tasks and results of the project, that are:

- The magnitude of the horizontal diffusion coefficient under various conditions is determined using both theoretical formulations and experimental results (Task 1);
- The numerical diffusion associated with the three schemes of interest is quantified (Task 2);
- The results of Tasks 1 and 2 are combined to yield the horizontal diffusion module for incorporation into SAQM (Task 3); and,
- SAQM is exercised with the new formulations and compared to existing model results for the various schemes, to determine the sensitivity of model results to specification of the horizontal diffusion coefficient (Task 4).

Appendix A contains reprints of two technical papers prepared during the duration of the project. These papers provide many of the equations and other background that was necessary to successfully complete the project. Appendix B documents revisions to the SAQM code resulting from this project.

2. HORIZONTAL TRANSPORT AND DIFFUSION

2.1 Representation of Horizontal Advection and Diffusion in Grid Models

The advection and diffusion of a concentration field C is described by the partial differential equation (PDE):

$$\frac{\partial C}{\partial t} + \nabla \bullet [VC - K\rho\nabla(C/\rho)] = 0 \qquad (2)$$

where **V** is the vector wind field, K is the diffusivity tensor of rank 2, and ρ is the atmospheric density, which is included so the diffusion process is properly driven by the gradient in the dimensionless mixing ratio, C/ρ. Within the framework of a grid model this PDE must be solved numerically. The significant role of non-linear processes within a photochemical model is responsible for the need for space discretization or gridding and, because the fields to be advected are known at only a finite number of points, errors develop during the transport process. The process of operator splitting then forces a genuine time discretization into the modeling. Time discretization also introduces errors; however, these are not as bothersome for two reasons. First, reducing the time step Δt increases the computer time proportional to $(\Delta t)^{-1}$, whereas reducing the mesh size Δx increases computer time and the required storage by a factor proportional to $(\Delta x)^{-2}$. Second, because operator splitting already limits the accuracy of the time-marching scheme to second order, efforts to retain higher-order temporal accuracy in individual advection steps have questionable value.

All of the horizontal advection solvers considered in this SAQM enhancement study are explicit, forward-in-time, high-spatial order (4th order accurate or better) methods. The current SAQM horizontal diffusion methodology is also explicit and forward-in-time, which is appropriate given the small size of the horizontal non-dimensional diffusivities, k (i.e., $k \equiv K \cdot \Delta t/(\Delta x)^2 << 0.25$) on these larger spatial scales. The concentration gradients estimated for use in SAQM's diffusion module are first-order accurate in space, as they simply involve the differences of grid-point concentrations -- a methodology that is both standard and adequate for the purpose.

2.2 Determination of the Magnitude of the Horizontal Diffusion Coefficient

A major limitation of representing atmospheric diffusion with Eq.(2) is that use of a temporally-constant diffusivity, K, generally limits one to plume growths that are proportional to the square root of transport time, t, in direct contrast with the nearly linear growth rates that are observed in nature (Hanna, 1994). A major reason for the masking of the anticipated transition to $t^{1/2}$ growth, for travel times longer than any reasonable estimate of a lateral turbulence Lagrangian time scale, is the combined effect of wind directional shear with height and vertical mixing. Moran's (1992) extensive dissertation on mesoscale atmospheric dispersion, including simulation of the long-range transport, Great Plains and CAPTEX tracer experiments using RAMS (Pielke et al., 1992), concludes that "horizontal dispersion can be enhanced and even dominated by vertical wind shear through either the simultaneous of delayed interaction of horizontal differential advection and vertical mixing..." Knowing that the vertical wind shear (e.g., turning of the wind with height) is built into the MM-5 wind fields, one must now ask:

a) How should the lateral turbulence in a directional-shear-free atmosphere be modeled; and
b) How well does MM-5 emulate the shears in the atmosphere?

Assuming presently, that wind shear effects are accounted for by MM-5, one must ask where appropriate mesoscale diffusivities are to be found. Plume growth rates measured in tracer experiments can not, of course, directly isolate the diffusive and wind shear contributions of the atmosphere; although, model dependent analyses of such experiments could. An alternative approach might involve use of an LES model in a shear-free atmosphere. We have alternatively used the Kinematic Simulation Particle (KSP) model (Yamartino, et al., 2000) to simulate plume growth rates in a shear-free flow. Figure 2-1 shows total and relative diffusion plume sigmas for a 100m elevated, point source release. Particles were released in clusters of 10 every 20 seconds for one hour. These clusters then evolve in a steady, D stability atmosphere with $u^* \approx 0.5$ m/s. For a plume having a standard deviation of order 10 km, lateral diffusivities of order $K_{yy} \approx u^* \cdot \sigma_y \approx 5000$ m^2/s are extracted for the relative diffusion and may be appropriate for inclusion into the lateral diffusion module of the SARMAP air quality model.

Generalizing this result to a grid where $\sigma_y = \Delta x/(2\cdot\pi)^{1/2}$, and assuming $\sigma_v \approx 2\cdot u^*$, one would estimate the lateral diffusivity to be:

$$K_{yy} \approx 0.2 \cdot \sigma_v \cdot \Delta x \qquad (3a)$$

and its non-dimensional equivalent to be:

$$K_{yy} \approx 0.2 \cdot (\sigma_v/u) \cdot \varepsilon \qquad (3b)$$

where $i_y = (\sigma_v/u)$ is the lateral turbulent intensity and $\varepsilon = u\cdot\Delta t/\Delta x$ is the Courant number.
In order to utilize Eqs.(3a) or (3b), one requires either measured σ_v or a comprehensive, micro-meteorological based model of σ_v that can be inserted into SAQM. The σ_v model chosen is taken from the KSP (Yamartino et al., 1998) and LASAT (Janicke,1995) models and is based on the micrometeorological relations of Gryning et al., 1987. The specific simplified equations used are:

$$\sigma_v = 2.0 \cdot u^* \cdot (1 - z/H)^{3/4} \quad \text{for stable (i.e., } L > 0) \qquad (4a)$$

and

$$\sigma_v = 2.0 \cdot u^* \cdot (1 - z/H)^{1/2} \quad \text{for unstable (i.e., } L > 0) \qquad (4b)$$

where L is the Monin-Obukov length and H is the mixed layer depth. One also notes that the coefficient of 2.0 that is used is not far from the value of 2.06 recently suggested by Nasstrom et al. (2000); though, it is clear from the recent work of Mahrt (2000), that the value of this coefficient should also depend on the averaging time implied by the air quality model's meteorological field update frequency.

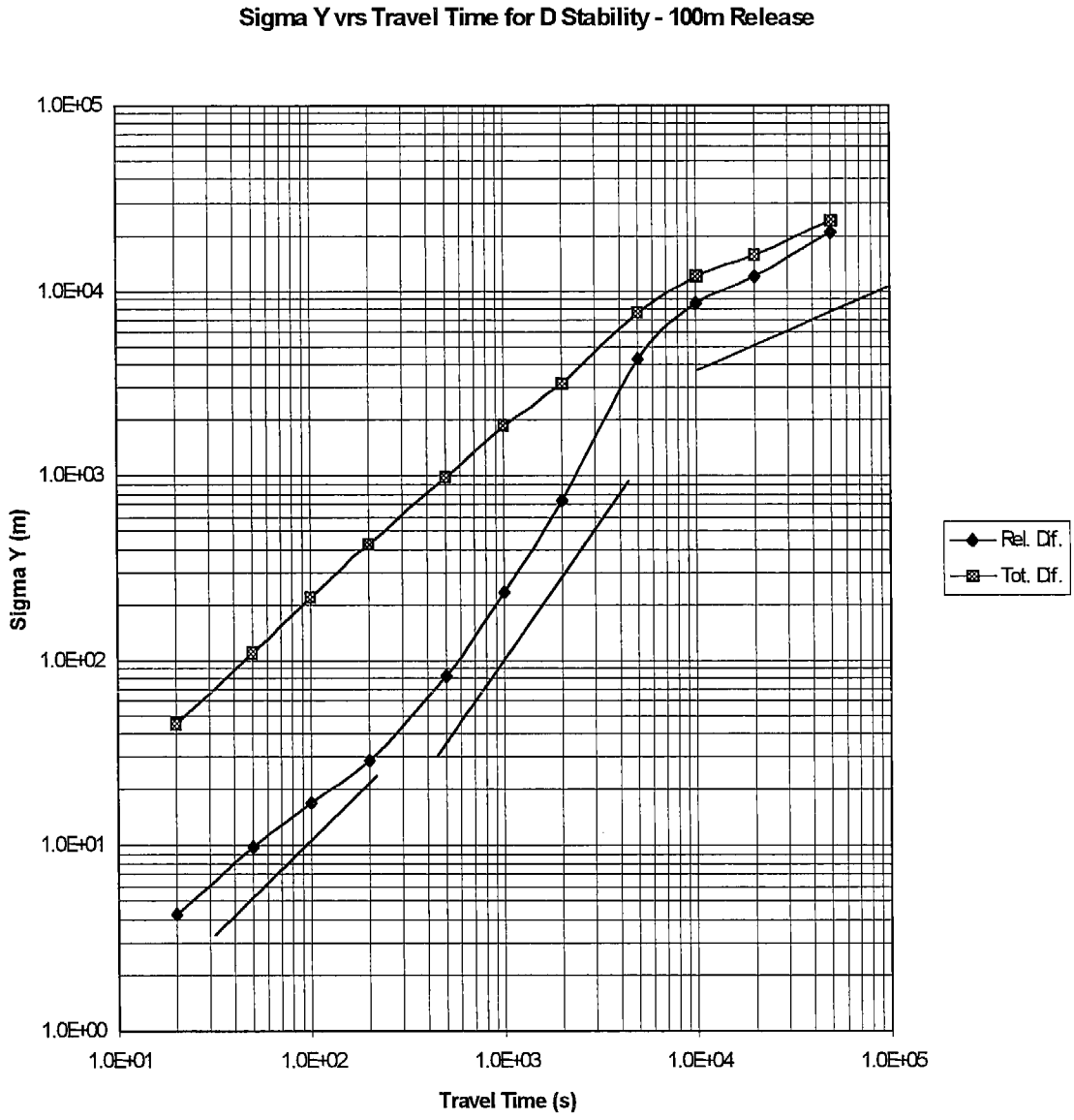

Figure 2-1. KSP generated total and relative diffusion estimates for 180 clusters of 10 particles released from a 100m non-buoyant source into a neutral, shear- free atmosphere. Accompanying lines indicate growth rates of t, $t^{3/2}$, and $t^{1/2}$.

The empirically derived Eq.(3a) can also be obtained from equating the long-time limit form of Taylor's (1921) statistical theory with the K theory relation of Batchelor (1949),

$$\sigma_y^2 = 2 \cdot \sigma_v^2 \cdot t \cdot T_L = 2 \cdot K_{yy} \cdot t \qquad (5)$$

where t is travel time and T_L is the Lagrangian time scale. This then yields the expression for the lateral diffusivity K in terms of σ_v and T_L as:

$$K_{yy} = \sigma_v^2 \cdot T_L \qquad (6a)$$

where T_L is now modeled as being proportional to a length scale, Δx, divided by the velocity scale, σ_v, dissipating an eddy of this length scale. Thus one obtains,

$$K_{yy} = C_v \cdot \sigma_v \cdot \Delta x \qquad (6b)$$

where C_v is an unspecified constant of proportionality. Injecting the empirical relation, $\sigma_y = 0.5 \cdot t$, from Pack (1978) and Heffter (1980), one might infer a $C_v \approx 0.5$ for absolute diffusion, and guess at value several times smaller for relative diffusion. However, there is no absolute or firm guidance with respect to choosing C_v here, due basically to the excessively wide range of Lagrangian time scale estimates (e.g., 600s and up) for lateral turbulence. As an additional conjectural constraint, one notes that Δx of 4-12km and $\sigma_v \approx 0.5$ m/s would yield T_L of C_v times $8\text{-}24 \cdot 10^3$ s. Limiting T_L to the one-hour, meteorological data update rate, would then imply C_v in the range of 0.15 to 0.45, so perhaps the KSP suggested value of $C_v \approx 0.2$ is not unreasonable.

2.3 Evaluating the Role of Wind Shears

Several mesoscale, photochemical models have long recognized the significance of wind shear in dispersing the pollutants and have attempted to include its effects through the use of the Smagorinsky (1963) stress tensor in the model's mesoscale diffusivity. For example, the CALGRID model (Yamartino, et al., 1992) uses the Smagorinsky formulation

$$K_S = \alpha_o^2 |D| (\Delta x)^2 \qquad (7a)$$

where $\alpha_o \approx 0.28$ and $|D|$ is the absolute value of the stress tensor, specified as,

$$|D| = \left[\left(\frac{\partial v}{\partial x} + \frac{\partial u}{\partial y} \right)^2 + \left(\frac{\partial u}{\partial x} - \frac{\partial v}{\partial y} \right)^2 \right]^{1/2} \qquad (7b)$$

to characterize the impact of stress in the wind field. Of course, if there are no velocity gradients or the wind field generator is incapable of simulating or maintaining these gradients, the approach has greatly reduced value. While the shear related corrections to horizontal transport in the SAQM will be advective rather than diffusive (as detailed in Section 3), the question of velocity gradient fidelity by the wind field generator remains a valid concern. Seaman (1998, private communications) has indicated that the gridded nature of MM-5 coupled with the properties of it's numerical algorithms can preserve only those spatial structures that exist over "several grid cells or more". Hence the model for diffusivity should consider those strong, near-surface wind gradients lost by MM-5.

Figure 2-2 shows a plot of the fraction of the mean surface wind residual that is explained by MM-5 over the 5-day episode of August 2-7, 1990. A value of 1.0 would indicate that the MM-5 field predicts the surface observations exactly, while a value of 0.0 could be achieved by having all MM-5 winds set to 0.0, so as to not influence the residual. A negative value indicates that the MM-5 predictions are worse than no prediction at all and could result from MM-5 predicting the wind flow in the opposite direction. Figure 2-2 shows that, after a short spin-up period, MM-5 predictions account for about half of the residual for the first three days, but that after this time the predictive power deteriorates rapidly. During the last two days, the MM-5 winds yield near-zero to negative skill fractions; suggesting that the model should have been re-initialized to obtain more realistic wind fields.

Figure 2-3 shows the ability of the 4-km resolution MM-5 winds to reproduce observed non-dimensional wind shears, (i.e., effectively $(dU/dX)*(\Delta X/U)$), for four intervals of station separation: 6-12km, 12-18km, 18-24km and 24-30km. As expected, one sees better performance (i.e., an Average Predicted/Average Measured ratio of 1.0 is ideal), for increased station separations. This is because the model is unable to reproduce detail associated with waves shorter than 'several' ΔX. The peaks tend to occur in the morning, before significant daytime convective activity, and the minima occur in the early evening, just after the cessation of convective activity. This behavior is seen consistently, but is not fully understood. Nevertheless, the fact that MM-5 can capture 60-80% of the shear, suggests that the shear corrections to transport based on MM-5 winds should have roughly the correct magnitude, and permits use of the shear formalism developed in Section 3.

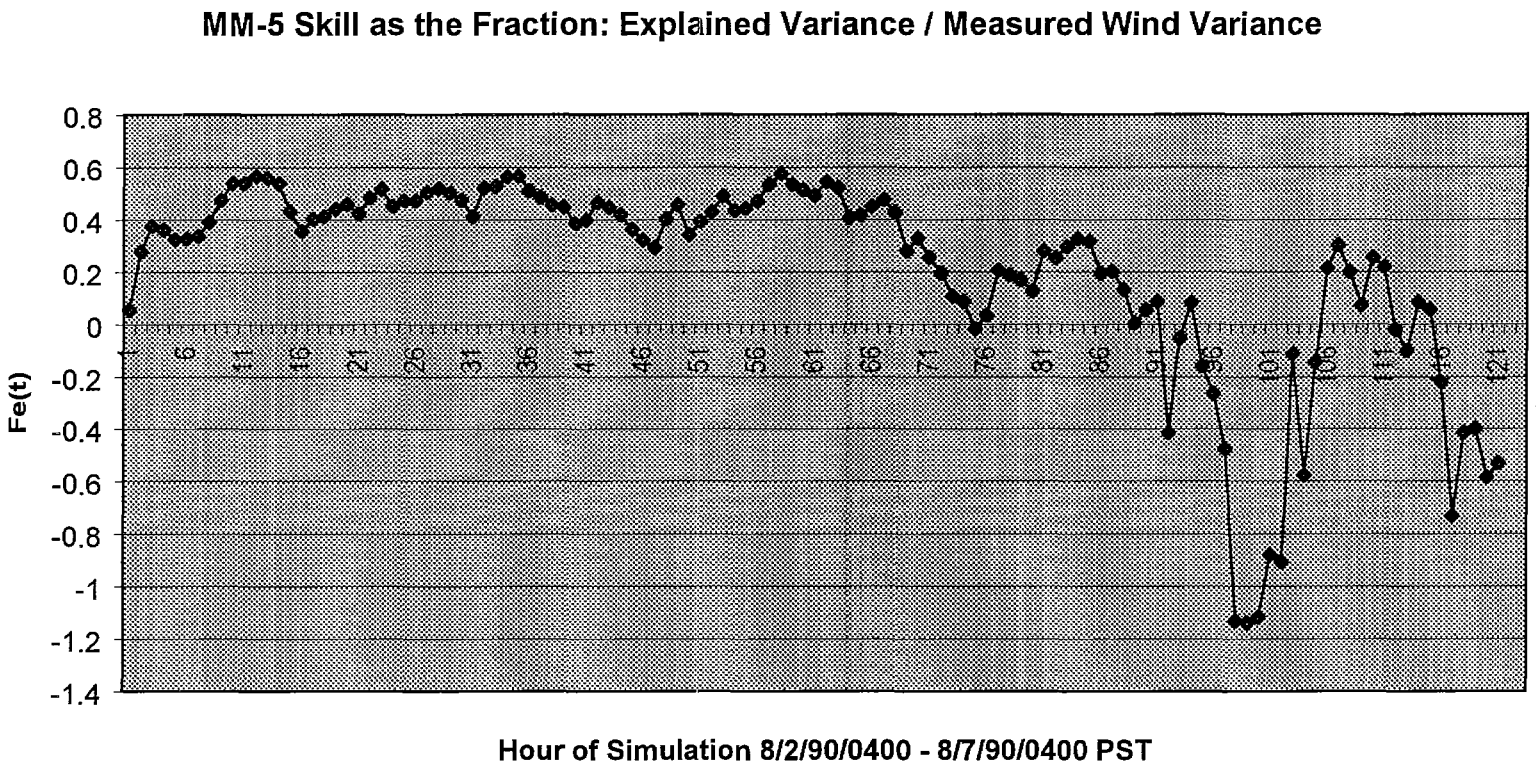

Figure 2-2. MM-5 explained variance normalized by the variance of the measured surface winds as a function of time during the August 2-7, 1990 SJVAQS episode.

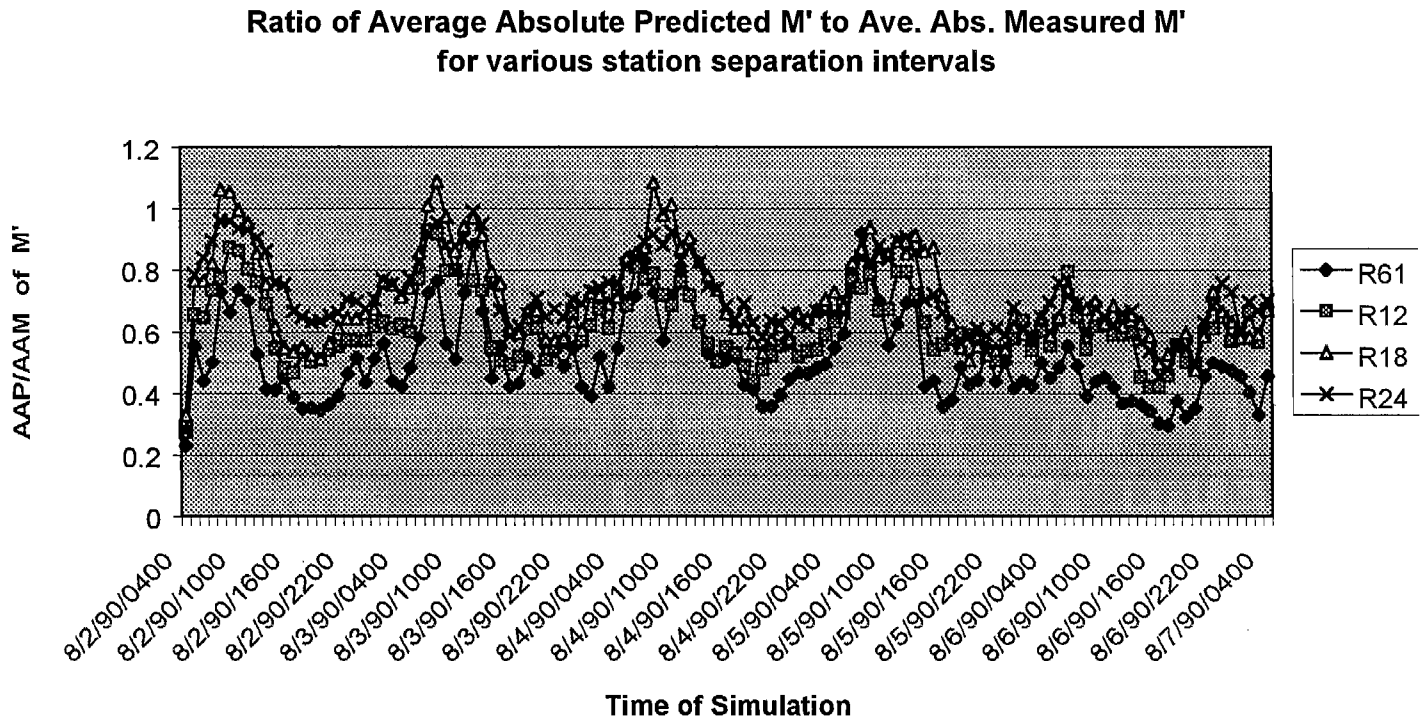

Figure 2-3. Ratio of the average absolute MM-5 non-dimensional shear measure M' (see text) to the average absolute, non-dimensional, measured surface wind shear as a function of time during the August 2-7, 1990 SJVAQS episode.

3. ERRORS AND CORRECTIONS IN HORIZONTAL TRANSPORT

3.1 Advection Scheme Choices, Characteristics and Constraints

Numerous papers have been written describing the theoretical stability characteristics and actual performance of different advection schemes. Roache (1976) provides an extensive introduction to the subject. Published intercomparisons of advection schemes (e.g., Long and Pepper (1976, 1981), Pepper et al. (1979), Chock and Dunker (1982), Schere (1983), Yamartino and Scire (1984), Chock (1985, 1991), van Eykeren et al. (1987)) are far from unanimous in their conclusion of the best overall scheme, but some consensus is emerging with respect to several considerations:

- It is important to conduct numerous tests, such as short- and long-wavelength fidelity and moments conservation tests, grid transmission tests, and point source tests, in one and two dimensions. Schemes showing superb fidelity with one test can show disastrous properties in another test.

- The constraint exists that implementation into a model with non-linear operators (e.g., second-order chemistry) and via operator splitting makes it conceptually difficult, if not impossible, to implement a time marching scheme more sophisticated than the Euler method (i.e., first order)*.

- Progressively higher order spatial accuracy rapidly encounters a "diminishing returns" plateau if one is limited to Euler time marching.

The Odman et al. (1996) report, *Horizontal Advection Solver Uncertainty in the Urban Airshed Model*, identifies three solvers that are most appropriate for photochemical modeling. These solvers were then made available as alternative solvers for use within the SAQM:

(1) Bott's (1989) area-preserving flux form (APF) algorithm. This fourth-order scheme is based on generalizations of the Crowley (1968) approach by Tremback et al. (1987), followed by a flux renormalization to ensure positive definite concentrations. This method yielded some unacceptable concentration over/undershoots that were eliminated in a more stringent monotone flux limiter version (MAPF) (Bott, 1992, 1993); however, the newer schemes are somewhat more diffusive.

(2) Yamartino's (1993) spectrally-constrained, Blackman cubic scheme. This Crowley-type scheme uses a polynomial expansion of within-grid-cell concentrations coupled with formulations of the derivatives that involve a blend of local and global definitions. These polynomials are then further constrained by

* A high-order time marching scheme is possible in the absence of the operator splitting associated with the method of fractional steps. In such a case the whole system of equations would be marched at a rate acceptable to the chemical system and a high spatial-order scheme, such as pseudospectral, would then be very promising. Computing costs could, however, be very large.

bounds extracted from spectral theory (Blackman and Tukey, 1958) to suppress dispersive, short-wavelength components. The approach also renormalizes within-cell concentrations to ensure correct within-cell mass and contains a minimally diffusive filter. This algorithm is currently in use in the European RTM-like model REM-3 and is implemented in recent releases of the CALGRID model (Yamartino et al., 1989, 1992).

(3) The Accurate Space Derivative (ASD) scheme (also referred to as the Advective Spectral Density scheme) as recently improved by Chock (1991) and Dabdub and Seinfeld (1994). Built upon the earlier ASD techniques of Gazdag (1973), this method uses the spectral expansion of the concentration field (i.e., the highest-spatial-order expansion that a grid can support) as its engine. It then uses the Forester filter to reduce fast Fourier transform noise, dissipate high frequency ripples, and avoid negative concentrations, with a claimed minor performance degradation.

These three modern schemes all exhibit the following features:

- creation of small numerical diffusion,
- good transport fidelity in terms of phase speed, group velocity, and low shape distortion,
- prohibition of negative concentrations,
- ability to cope with space-time varying vertical level structures,
- mass conservation, and
- limitations on the creation of new maximum or minimum concentration values.

One additional feature, the ability to accommodate strong shear flows correctly, is generally not demanded of advection schemes, but can play an important role in the overall modeling process.

Satisfying some of the above constraints can cause deterioration in other aspects of a scheme's performance. For example, the avoidance of negative concentrations is often achieved via clipping or some other form of short-wavelength filtering. This in turn increases the effective numerical diffusivity of the scheme, but is considered a necessary performance price to pay, as the presence of negative concentrations would, among other problems, cause most chemistry solvers to fail. Mass conservation is another feature that one would expect in a regulatory model, and it is easy to guarantee in most flux formulations of the advection equation; however, some regulatory models have encountered problems conserving both mass and the constancy of a uniform mixing ratio field.

Finally, some authors (e.g., Hov et al., 1989; Odman and Russell, 1991) note that some minor limitations in the previously identified features can become more serious problems when the non-linear chemistry operator is included, as predicted concentrations are sensitive to bilinear species concentration products. Such problems are likely minimized by choosing or optimizing a scheme based on minimal residuals or chi-square considerations, rather than best peak value retention or some other non-optimal criterion. For example, adjustable coefficients within the Yamartino (1993) scheme can be changed to yield negligible numerical diffusion (or even anti-diffusion), but

the ensuing loss in accuracy may render this a dubious achievement.

3.2 Advection Scheme Performance and Numerical Diffusion

Numerical transport schemes are often tested using initial mass distributions that are dominated by the longer (e.g., $\lambda > 6 \cdot \Delta x$) wavelengths on the grid. Whereas such long wavelength propagation tests are essential, they tend to show an advection scheme at its minimally diffusive best. Adequate short wavelength performance is also extremely important in air quality simulation models and is more difficult to obtain. One of the most stringent tests involves the two-dimensional transport and diffusion of emissions from a single-grid-cell point source. Odman et al. (1996) perform this point source test for a variety of schemes at Courant (a.k.a. CFL) numbers of $\varepsilon_x = u \cdot \Delta t / \Delta x = 0.12$ and $\varepsilon_y = 0.12$. We repeated those tests for the ASD (Dabdub, 1994), Bott (1989), and Yamartino (1993) schemes and obtained the similar, though not identical results, shown in Table 3.1a. Some of the smaller differences found may be due to the way (i.e., during which operations) material is injected into the source cell; however, our tests find significantly improved results for the ASD scheme.

Table 3-1a. Fraction of Theoretical Plume Value Seen at CFL=0.12

Quantity/Scheme	ASD	Bott	Yamartino
Peak	0.786	0.956	1.03
cell (15,15)	0.767	0.636	0.745
cell (25,25)	0.763	0.563	0.643
Minimum value (Ideal is 5.0)	0.0	0.4	4.8

The test involves a single-cell point source at cell (5,5) having a source strength such that the centerline concentrations would be 100 downwind, were it not for numerical diffusion. The background concentration of 5.0 should appear throughout the grid and not be affected by the emissions from this point source, but the tabulated minimum values clearly show that both the ASD and Bott schemes "burn significant holes" into this background. This hole-burning effect can cause significant impacts to atmospheric chemistry in the near vicinity of major point sources and cannot be easily remedied without increasing the numerical diffusion of a scheme. Upon raising the Courant number to 1.0, which is acceptable to the Bott and Yamartino schemes but not the ASD scheme, and which should yield a perfect solution, we found that the emissions used in the tests of Odman et al. and Yamartino et al. (1989, 1992) were computed to be a factor of two too high, making the results overly optimistic. It was also found that the timing and split-up of the emissions injections relative to the various operators, made a significant impact on whether one could achieve the exact solution everywhere for ε=1 (i.e., at and near the source) and on the degree of background "hole burning" observed.

Using the corrected emissions, this point test was then repeated at Courant numbers of 0.12 and 0.5, and results are presented in Tables 3.1b and 3.1c, respectively.

Table 3-1b. Corrected Fraction of Theoretical Plume Value Seen at CFL=0.12

Quantity/Scheme	ASD	Bott	Yamartino
cell(5, 5)	0.357	0.537	0.430
cell (6, 6)	0.392	0.450	0.517
cell (15,15)	0.379	0.326	0.380
cell (25,25)	0.383	0.292	0.330
Minimum value (Ideal is 5.0)	1.9 (1 cell from bc) 3.1 elsewhere	0.3	5.0

Table 3-1c. Corrected Fraction of Theoretical Plume Value Seen at CFL=0.50

Quantity/Scheme	ASD	Bott	Yamartino
cell(5, 5)	0.626	0.671	0.641
cell(6, 6)	0.480	0.555	0.629
cell (15,15)	0.370	0.374	0.505
cell (25,25)	0.324	0.334	0.413
Minimum value (Ideal is 5.0)	1.3 (1 cell from bc) 3.1 elsewhere	0.8	4.4

The "hole-burning" is present at both Courant numbers and is most serious for the Bott scheme and for ASD very near the boundary cell, where ASD is known to have some problems.

This point source test is also useful for extracting numerical diffusivities associated with point source plume diffusion. Assuming Fickian diffusion and a Gaussian-shaped plume of initial dimension $\sigma_y(0)=\Delta x/(2\cdot\pi)^{1/2}$ and subsequent growth according to the relation, $\sigma_y(t)= 2\cdot K\cdot t + \sigma_y(0)^2$, with $t=n\cdot\Delta x/u$, one can show that the non-dimensional numerical diffusivity, $k_N \equiv K\cdot\Delta t/(\Delta x)^2$, can be estimated as:

$$k_N = \left[\left(\frac{C(0)}{C(n\,\Delta x)}\right)^2 - 1\right]\frac{\varepsilon}{4\pi\, n} \qquad (8)$$

Determination of such numerical diffusivities was carried out (Yamartino et al., 1989, 1992) for CALGRID's original chapeau function scheme, so that stability-dependent atmospheric diffusivities could be added in to achieve realistic diffusion for plumes a few cells wide. Such an approach is not inconsistent with the goals of this project; however, this study requires a more detailed model for the numerical diffusivity.

The normalized concentration values one grid cell downwind of the source are found from Eq. (8) to yield the highest diffusivities at each Courant number and these values are presented in Table 3-2 below.

Table 3-2. Peak Non-dimensional Plume Diffusivity Estimated from Equation(8) for Cell (6,6)

Scheme/CFL	0.12	0.5
ASD	0.053	0.133
Bott	0.038	0.089
Yamartino	0.026	0.061

The single-cell point source is perhaps the most severe, yet highly relevant test that one can apply to an advection scheme destined for use in an air quality grid model. The only more severe test involves advection of the $\lambda = 2{\cdot}\Delta x$ wave, which is nothing more than the transport of a pattern of alternating ones and zeros. One time step of marching the $2{\cdot}\Delta x$ wave pattern at $\varepsilon = 0.5$ will always yield a result of 0.5 everywhere, and for all schemes, and corresponds to a non-dimensional diffusivity, $k_N = 0.25$, the largest value that exists, or need exist, in forward-in-time, explicit diffusion schemes. This finite upper bound on value of k_N is useful and is contrasted with the infinite diffusivies that one can obtain (e.g., see Odman et al., 1996) from the analytic Fourier analyses of diffusion in transport schemes. This is not to discredit the value of such Fourier analyses, as they also yield valuable insights into the wavenumber and Courant number dependencies of such diffusivities, but the absolute value of the diffusivities so obtained must be adjusted if they are to be used in a numerical diffusion module. In fact, such analyses teach us to expect ε dependencies of the type $[4{\cdot}|\varepsilon|{\cdot}(1 - |\varepsilon|)]^p$ and wavelength dependencies proportional to λ^{-n} for schemes that are n^{th} order accurate in space.

Keeping these results in mind, we return to longer wave tests of the transport schemes. In particular, we conducted 1-d tests of advection of a cosine wave pattern for two time steps: one forward step of size $+\varepsilon$ followed by a backward step of $-\varepsilon$. In the case of no diffusion, one obtains the original pattern back, and such was the case for all ASD tests for $\lambda \geq 4{\cdot}\Delta x$. Unlike the ASD, which uses cosines (and sines) as its basis functions, the other schemes are not 'tuned' perfectly to cosines and yield, after a small amount of algebra, finite diffusivities. Figure 3-1 presents the non-dimensional diffusivities for the case of the $\lambda = 4{\cdot}\Delta x$ wave superimposed on top of a finite background.

Figure 3-1 shows: (a) that the diffusion from the Bott and Yamartino schemes is comparable for the $4{\cdot}\Delta x$ wave; (b) that both show diffusivities far below that of the low-order donor cell method; and (c) that both are reasonably modeled by the simple curve, $k_N = 3.5{\cdot}10^{-3} \cdot [4{\cdot}|\varepsilon|{\cdot}(1 - |\varepsilon|)]$. Other test at larger wavelengths indicated that these schemes showed a λ^{-4} falloff in diffusivity, which is expected for schemes, such as Bott and Yamartino, which are fourth-order accurate in space.

In yet other long-wave tests, such as the classic $\lambda = 8 \cdot \Delta x$ cosine hill rotation test (Chock and Dunker, 1982), we determined the diffusivity needed to diffuse the ASD method (with its 2-revolution maxima of 99%) down to the peak height levels of 73%, obtained by both Bott and Yamartino schemes. The result of these and other tests was a numerical diffusivity approximation for these two schemes that can be expressed as:

$$k_N = 0.025 \cdot (3 \cdot \Delta x / \lambda)^4 \cdot \; [4 \cdot |\varepsilon| \cdot (1 - |\varepsilon|)] \qquad (9).$$

for $\lambda \geq 3 \cdot \Delta x$. For shorter λ the expression, $(3 \cdot \Delta x / \lambda)^4$ is bounded by 1.0.

The next question is where does one obtain a measure of λ from an arbitrary concentration distribution as found on the grid of a typical photochemical model simulation. The answer is that one doesn't find λ directly, but rather λ^{-4}, which is just proportional to the fourth derivative of the local concentration distribution and directly related to the truncation error of these numerical schemes. This relationship between the fourth derivative and λ^{-4} can be seen by considering the Fourier wave, $y = A \cdot \cos(2 \cdot \pi \cdot x / \lambda)$. The fourth derivative of y by x, divided by the function itself, yields the desired relationship: $y^{(4)} / y = (2 \cdot \pi / \lambda)^4$.

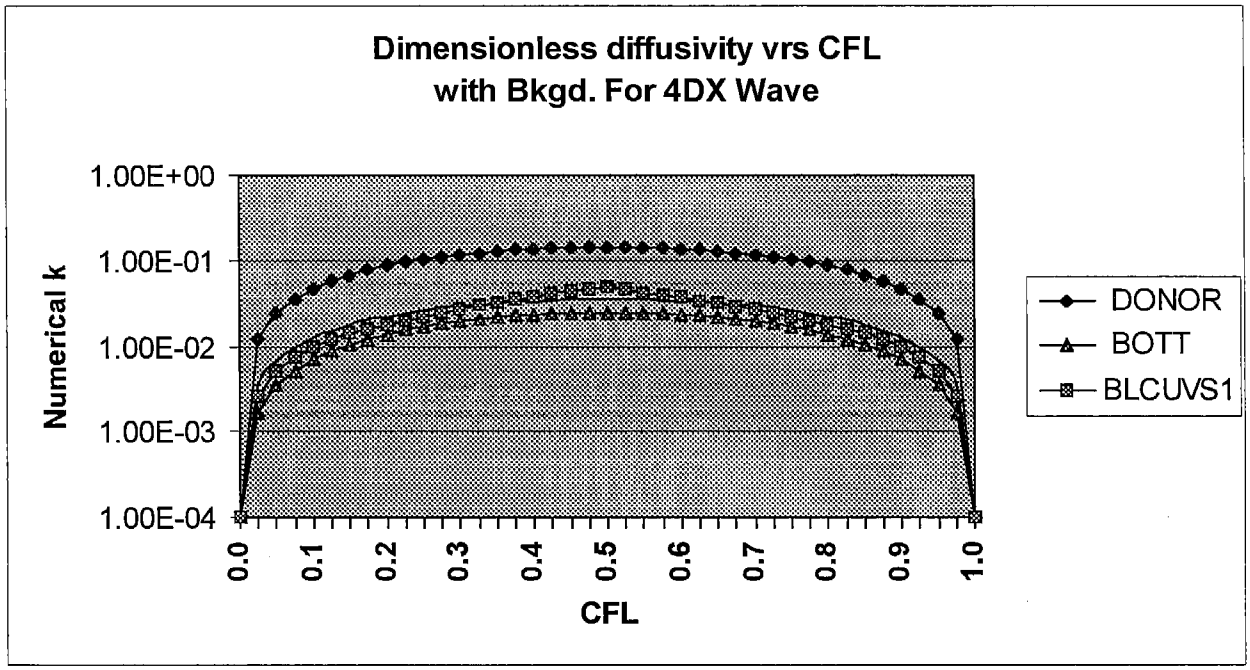

Figure 3-1. Non-dimensional diffusivities, k_N, versus Courant number for the $\lambda = 4 \cdot \Delta x$ wave. Also shown as a solid line is the curve $k_N = 3.5 \cdot 10^{-3} \cdot [4 \cdot |\varepsilon| \cdot (1 - |\varepsilon|)]$.

3.3 Correction for Artificial Diffusion

"Artificial" diffusion refers to the instantaneous dilution of emissions and concentrations by the finite volume, $\delta V = \Delta x \cdot \Delta y \cdot \Delta z$, of the grid cells. This instantaneous diffusion has traditionally either been ignored or, if the sources contributing to this cell of volume, δV, are deemed important enough, treated by:

a) a finer nested mesh to cover the sub-domain of interest, or
b) a plume-in-grid (PiG) module to describe the early dispersion/chemistry evolution of pollutants emitted by one or a few sources.

If one does not wish to incur the computational expense, added complexity, and unresolved scientific issues (e.g., use of simplified chemistry in PiGs, 1-way vs 2-way nested grids) surrounding either of these approaches, one must accept this initial dilution into the volume, δV. However, there are considerations one may take into account in deciding on the "actual" amount of horizontal diffusivity to be used in SAQM. As indicated previously, the basic goal of this study is to determine all the processes in the atmosphere that lead to the "total" horizontal diffusion or smearing of material in nature, and then represent the SAQM's "actual" horizontal diffusion coefficient as: actual = total - (numerical + artificial). If the sources within volume, δV, predominate over the material advected into this cell, this will show up as a "sharpening or peaking" of the concentration distibution, which in turn will be seen as a lowering of the effective local wavelength of the concentration distribution toward the minimum value of $\lambda = 2 \cdot \Delta x$ (or Δy or Δz). For example, one could use the criteria, $\lambda < 3 \cdot \Delta x$, to decide that enough artificial diffusion has already occurred, so that the "actual" diffusion should be set to zero. This approach, while intellectually appealing, has not been tested due to the currently poor and unpredictable response of most of the present advection schemes (e.g., the Bott and ASD schemes) to transporting these short wavelengths. That is, the use of some "actual" diffusion can serve as a "preemptive strike" against the even worse numerical diffusion associated with short wavelength distributions.

Consistent with these short wavelength transport problems, it may actually be beneficial to apply filtering (e.g., the Forester filter used in ASD) before transport step rather than after transport, as is currently done in nearly all transport algorithms.

3.4 Inclusion of Wind Shear Effects

In order to account for diffusion due to distortion or stress in the horizontal wind field, the CALGRID model used the moderately simple Smagorinsky (1963) formulation of Eq.(7) to characterize and simulate the stress in the wind field. The K_S of Eq.(7) can be computed directly from the already existing u, v horizontal wind field components. In his review of horizontal diffusion processes and their representation, Hanna (1994) points out the problem that "horizontal diffusion follows a linear growth rate with time for travel times out to a day or more" whereas K-theory diffusion leads to $t^{1/2}$ plume growth. This fact stresses the importance of capturing as much as possible of the wind field shear in the advective portion of the transport flux vector, F, given as

$$F = VC - K\rho\nabla(C/\rho) \quad ; \tag{10}$$

unfortunately, this cannot be done for the scales that are smaller than Δx. For these smaller scales we first consider the problem of u (i.e., x) transport through the face of a single grid cell. One then may write the local flux as either an advective flux,

$$F_a = \left[u + \left(\frac{\partial u}{\partial y}\right) y + \left(\frac{\partial u}{\partial z}\right) z \right] \left[C + \left(\frac{\partial C}{\partial y}\right) y + \left(\frac{\partial C}{\partial z}\right) z \right] \tag{11}$$

or as a diffusive flux,

$$F_d = -\rho \left[K_{xx} \left(\frac{\partial (C/\rho)}{\partial x}\right) + K_{xy} \left(\frac{\partial (C/\rho)}{\partial y}\right) + K_{xz} \left(\frac{\partial (C/\rho)}{\partial z}\right) \right] \tag{12}$$

Integrating Eqs. (11 and 12) over the facial area $\Delta y \cdot \Delta z$ of the cell, and noting that the u·C term is the purely advective term already handled by the advection scheme and the term containing K_{xx} is the traditional diffusion term, the matching of terms enables one to extract expressions for the K tensor elements, such as:

$$K_{xy} = -\frac{(\Delta y)^2}{12} \left[\left(\frac{\partial u}{\partial y}\right)\left(\frac{\partial C}{\partial y}\right) \right] / \left[\left(\frac{\partial C}{\partial y}\right) - \frac{C}{\rho}\left(\frac{\partial \rho}{\partial y}\right) \right] \tag{13a}$$

and

$$K_{xz} = -\frac{(\Delta z)^2}{12} \left[\left(\frac{\partial u}{\partial z}\right)\left(\frac{\partial C}{\partial z}\right) \right] / \left[\left(\frac{\partial C}{\partial z}\right) - \frac{C}{\rho}\left(\frac{\partial \rho}{\partial z}\right) \right] \tag{13b}$$

which in the case of negligible density variation become

$$K_{xy} = -\frac{(\Delta y)^2}{12} \left(\frac{\partial u}{\partial y}\right) \tag{14a}$$

and

$$K_{xz} = -\frac{(\Delta z)^2}{12} \left(\frac{\partial u}{\partial z}\right) \tag{14b}$$

Extension to the y flux-related tensor components K_{yx} and K_{yz} is straightforward and the similarity between Eqn (14) and Eqn (7) becomes more striking when one realizes that $\alpha_o^2 = (0.28)^2 = 1/12.8$ or $\alpha_o^2 \cong 1/12$. Further, what this comparative analysis shows is that:

- rather than use the directionally blind K_S for wind shear-related lateral "diffusion" in both directions x and y, one may now selectively employ the direction-specific tensor elements K_{xy} and K_{xz} for x exchange fluxes and K_{yx} and K_{yz} for y exchange fluxes, respectively;

- unlike in the directionally blind K_S, where only the diagonal diffusivities, such as K_{xx}, are impacted and hence where x direction fluxes are purely diffusive and proportional only to $(\partial C/\partial x)$, inclusion of these off-diagonal terms can result in x diffusive fluxes to be driven by gradients $(\partial C/\partial y)$ and $(\partial C/\partial z)$. While seemingly counterintuitive, one must recall that we are not modeling actual diffusion with these off-diagonal terms, but rather the influence of wind shears on mass transfer;

- unlike in the directionally blind K_S, the divergence related terms, $(\partial u/\partial x)$ and $(\partial v/\partial y)$, will not appear in the four K tensor elements. Rather, these terms can and should instead be included in the wind gradient correction to any Crowley integral-flux advection scheme. This correction (Yamartino, 1998) amounts to replacing the one-dimensional Courant number, ε, with the corrected $\varepsilon' = \varepsilon \cdot [1 - \exp(-a)]/a$, where $a=(\partial \varepsilon/\partial x)$. Such a correction correctly pinpoints the "last molecule" destined to leave the grid cell during the advection step and is consistent with Emde's (1992) correction for Lagrangian back trajectories; and

- unlike the Smagorinsky K_S, the lateral diffusivities will now include corrections for the variation in winds u and v between vertical levels via terms K_{xz} and K_{yz} respectively.

While the above outlined approach certainly appears more promising than the traditional Smagorinsky formulation, analyses of the SAQM code indicated that it would be far more practical to implement shear using the advective representation (i.e., Eq.(11)) rather than as off-diagonal diffusion terms. In addition, consistent treatment of second-order terms called for expansion of Eq.(11) to:

$$F_a = [\, u + u_y \cdot y + u_z \cdot z + (u_{yy} \cdot y^2 + u_{zz} \cdot z^2) / 2 \,] \cdot [\, C + C_y \cdot y + C_z \cdot z + (C_{yy} \cdot y^2 + C_{zz} \cdot z^2) / 2 \,] \quad , \qquad (15)$$

where subscripts denote differentiation here. Expanding Eq.(15) and integrating over the facial area $\Delta y \cdot \Delta z$ of the cell, one obtains the integral average advective flux as:

$$\begin{aligned} \langle F_a \rangle = u \cdot C &+ [u_y \cdot C_y + (u_{yy} \cdot C + u \cdot C_{yy}) / 2 \,] \cdot (\Delta y)^2 / 12 \\ &+ [u_z \cdot C_z + (u_{zz} \cdot C + u \cdot C_{zz}) / 2 \,] \cdot (\Delta z)^2 / 12 \quad . \end{aligned} \qquad (16)$$

Studies with the prototype model indicated that inclusion of the $[u_y \cdot C_y + u_z \cdot C_z]$ term made negligible differences (e.g., $\pm$ 1 ppb) to the ozone, and given the resulting increases in CPU time for SAQM, the second derivative terms were not added in.

4. ADJUSTMENT OF THE HORIZONTAL DIFFUSION COEFFICIENTS IN SAQM

4.1 A Revised Horizontal Transport Scheme for SAQM

In the original SAQM, the lateral plume dispersion process was greatly simplified by assuming a space-time-invariant diffusivity $K_{xx} = K_{yy} = K_H$ of 50 m^2/s for the 12 km grid resolution domain. Conversion of this diffusivity to a non-dimensional atmospheric value of $k_a = K_H \cdot \Delta t/(\Delta x)^2$ yields a $k_a = 5.2 \cdot 10^{-5}$ for $\Delta x = 12$ km and $\Delta t = 150$ s, but this value is seen to be about two (or more) orders-of-magnitude smaller than the effective numerical diffusivities for sharply peaked distributions as presented in Table 3-2. Thus, inclusion of this 50 m^2/s lateral diffusivity into SAQM for the 12 km mesh produces negligible differences. Further examining the values in Table 3-2 and the relative centerline concentrations of Table 3-1, we note that plume dispersion begins to "look significant" relative to daytime dispersion rates at dimensionless diffusivities of order 10^{-2}. For the finer SAQM grid (i.e., $\Delta x = 4$ km and $\Delta t = 75$ s), this would correspond to diffusivities of about 2000 m^2/s and 10,000 m^2/s for the coarser 12km grid; thus, it is important to include the larger diffusivities corresponding to lateral diffusion in the atmosphere as well as correct for the numerical diffusion in the horizontal transport scheme. Both of these effects, and the additional correction for wind shears, have been incorporated into a revised SAQM modeling system. The modified and additional subroutines developed during this study can be brought into (or removed from) the operational SAQM simply by changing the mix of subroutines available at code compilation time. In practice, this is accomplished by having different "Make" files for the original and modified versions, and no other changes to data structures, formats, or input files are needed. Thus, no changes to SAQM's meteorological preprocessor or other SAQM file structures were instituted. Alternative modules are also available so that SAQM can be run with either the ASD, Bott, or Yamartino advection schemes; however, the need to run with such alternative advection schemes is lessened by the fact that, after correction for differing numerical diffusivities, the alternative schemes yield very similar results. A complete list and description of these new and modified subroutines is presented in Appendix B.

4.2 SAQM Sensitivity Tests

SAQM codes and input data files were provided by Dr. Saffet Tanrikulu of ARB for the August 3-6, 1990 SARMAP episode. In addition, the SAQM code provided contained the Bott advection scheme plus alternative modules for switching to the ASD or Yamartino schemes.

In preparation for testing the revised model algorithms, the 1-way no-PiG (Plume-in-Grid) 12 km and 4 km versions of SAQM that were received on tape from ARB were ported to the Earth Tech HP work station platforms and tested using the August 1990 episode. Several minor modifications were made to the code to allow SAQM to run on the HP. Comparisons were made to several other versions of SAQM that Earth Tech has and minor changes were made to update the chemical mechanism. The input files were downloaded from tape, the run scripts were modified, and both the 12 km and 4 km versions were exercised for several model days to test the porting of the software. The resulting ozone concentrations were reasonable in magnitude and temporal behavior, and other species also appeared to be reasonable.

Further investigation of the SAQM codes provided to Earth Tech revealed that they may not be the most current versions of SAQM. The codes provided were the PiG versions (both with PiG and without PiG) and the alternative advection scheme versions (Bott, ASD, Yamartino). None of these versions has the ability to produce hourly-average, ground-level concentration files. Furthermore, there were several changes to the CBM-4 routine codes that were made by SUNY Albany in 1996 that were not contained in these versions. Earth Tech inserted these chemistry changes to the reaction codes, but did not insert code changes to enable output of hourly-average concentrations (i.e., rather than 'snapshot') values. We are somewhat surprised that ARB relies on the end-of-hour 'snapshot' concentrations for its regulatory work, but presume that this is intentional.

As a first step to developing a modified SAQM, a more general version of the horizontal diffusivity routine, HDIFF, has been created and tested. The Bott scheme is used for most of the tests described in this section.

An initial sensitivity test was performed with the SAQM 12 km, CBM-4, non-PiG, 1-way version, in which the entire 5-day episode (2 through 6 August 1990) was run with the existing horizontal diffusivity scheme (i.e., 50.0 m^2/s times the nondimensionalizing factor [0.5 * DT / DX**2]), and then with an alternative algorithm that assumes a realistic, but significantly larger horizontal diffusivity of K = 1250.0(m) · U(m/s) (times the same nondimensionalizing factor), where $U = [u^2 + v^2 + 0.25]^{1/2}$. The horizontal diffusion from the alternative method should be about an order of magnitude larger (i.e., two orders of magnitude increase in K leading to an order of magnitude increase in plume spreading) than that from the original (Base Case) K=50. m^2/s implementation, though not as large as one of the currently-disabled alternatives that resides in the SAQM code and dates from sensitivity experiments performed during the 1980s on SAQM's predecessor, RADM.

The results of the sensitivity experiments were that increased horizontal diffusivities led to a decrease in maximum predicted daily ozone concentrations and also to a spreading out and diluting of the pollutant plumes, as represented by the two-dimensional maximum ozone concentration fields shown in the accompanying figures. Specifically, the figures show the August 5^{th} (Figure 4-1) and 6^{th} (Figure 4-2) daily maximum, Layer-1 ozone concentrations (ppb) from SAQM using the original, Base Case diffusivity assumption (Figs. 4-1a and 4-2a) and the increased diffusivity of this test (Sensitivity Case) algorithm (Figs. 4-1b and 4-2b). The decrease in the absolute maximum was seen on every day and ranged up to 11 percent. The location and time of occurrence of the maximum also sometimes changed somewhat. The horizontal diffusivity change also had impacts on whether the US EPA 1-hour ozone limit was exceeded and by how much, and, thus, would impact appropriate regulatory strategies.

Table 4-1. Comparison of maximum instantaneous ozone concentrations (ppb) and their time and location of occurrence for the original Base Case SAQM horizontal diffusion coefficient and an enhanced, wind speed dependent (Sensitivity Case) diffusivity.

	Base Case Diffusion			Sensitivity Test Case		
Date	Max O3	LST	Cell	Max O3	LST	Cell
8/2/90	119.3	14	11,31	114.8	15	13,31
8/3/90	129.2	16	19,27	120.4	15	17,27
8/4/90	128.0	16	18,26	113.6	16	18,26
8/5/90	130.9	14	25,20	123.9	12	24,20
8/6/90	143.2	14	25,20	131.5	14	25,20

Three additional simulations using the Bott scheme, plus the revised shear and diffusivity modules developed during this study, were also run. These began with the Base Case version of the model, but:

1. added the shear transport algorithm (Shear Case);

2. also substituted the Base Case diffusivity module for the new micrometeorological-based algorithm for lateral diffusivity (Shear + Sigma_V Case); and

3. further added the subtractive correction for numerical diffusion (Shear + Sigma_V - Num. Dif.) and is also referred to as the (All Case).

The results of these runs incorporating the new modules are displayed in the c,d,and e frames of Figs. 4-1 and 4-2, respectively, and their daily maximum ozone values are tabulated below in Table 4-2.

Table 4-2. **Comparison of maximum instantaneous ozone concentrations (ppb) for the five Bott cases described above plus the final shear and diffusion algorithm using the Yamartino and ASD advection schemes. It should be noted that the numerical diffusivity correction for ASD is zero.**

	BOTT					YAM	ASD
day	base	senstest	shear	shr_sv	all	all	all
214	119.3	114.8	119.8	117.2	117.1	116.5	109.1
215	129.2	120.4	129.0	120.6	120.9	119.8	118.0
216	128.0	113.6	127.9	114.4	114.4	114.1	116.8
217	130.9	123.9	132.2	114.9	115.2	117.6	109.6
218	143.2	131.5	143.9	128.4	129.3	126.9	124.9
CPU(hrs)	16.3	16.3	19.5	19.2	21.0	25.6	34.1

Focusing on the three "All" cases involving the sum of final modules for shear, diffusivity based on atmospheric velocity standard deviation estimates, σ_v, and a numerical diffusion correction for the Bott and Yamartino routines (n.b., the size of the correction for ASD was zero), one sees that the Bott and Yamartino results for the daily maximum ozone generally agree to within a few ppb, whereas the ASD results tend to be low by as much as 10%. This may be partially due to the fact that our primary correction for numerical diffusion is based on the scheme's diffusion of long-wave components. As ASD does not diffuse these longer waves, its numerical diffusivity correction was set to zero. In addition, ASD's spatial order accuracy is N/2, where N is the number of X or Y gridpoints, so that a λ^{-4} falloff in the numerical diffusion correction is inappropriate. However, ASD does significantly diffuse the shorter waves (i.e., $\lambda/\Delta x = 2,3$) and ignoring this potential correction may be partially responsible for these differences. On the other hand, if we use the Bott experience as a guide, subtraction of the numerical diffusion led to a rise in the maximum daily ozone of less than 1 ppb and, hence, is unlikely to account for all of the several ppb changes seen here.

Figure 4-3 shows the difference field of maximum daily ozone between the Bott and ASD schemes for the last day of the simulation (i.e., August 6). The fact that this difference field is "spikey", rather than smooth, lends further support to the notion that near-source differences in the dispersion of point source emissions (i.e., a single 12km cell -- which can represent a significant fraction of a small city's emissions) may play a significant role in explaining the differences seen in the ASD model results.

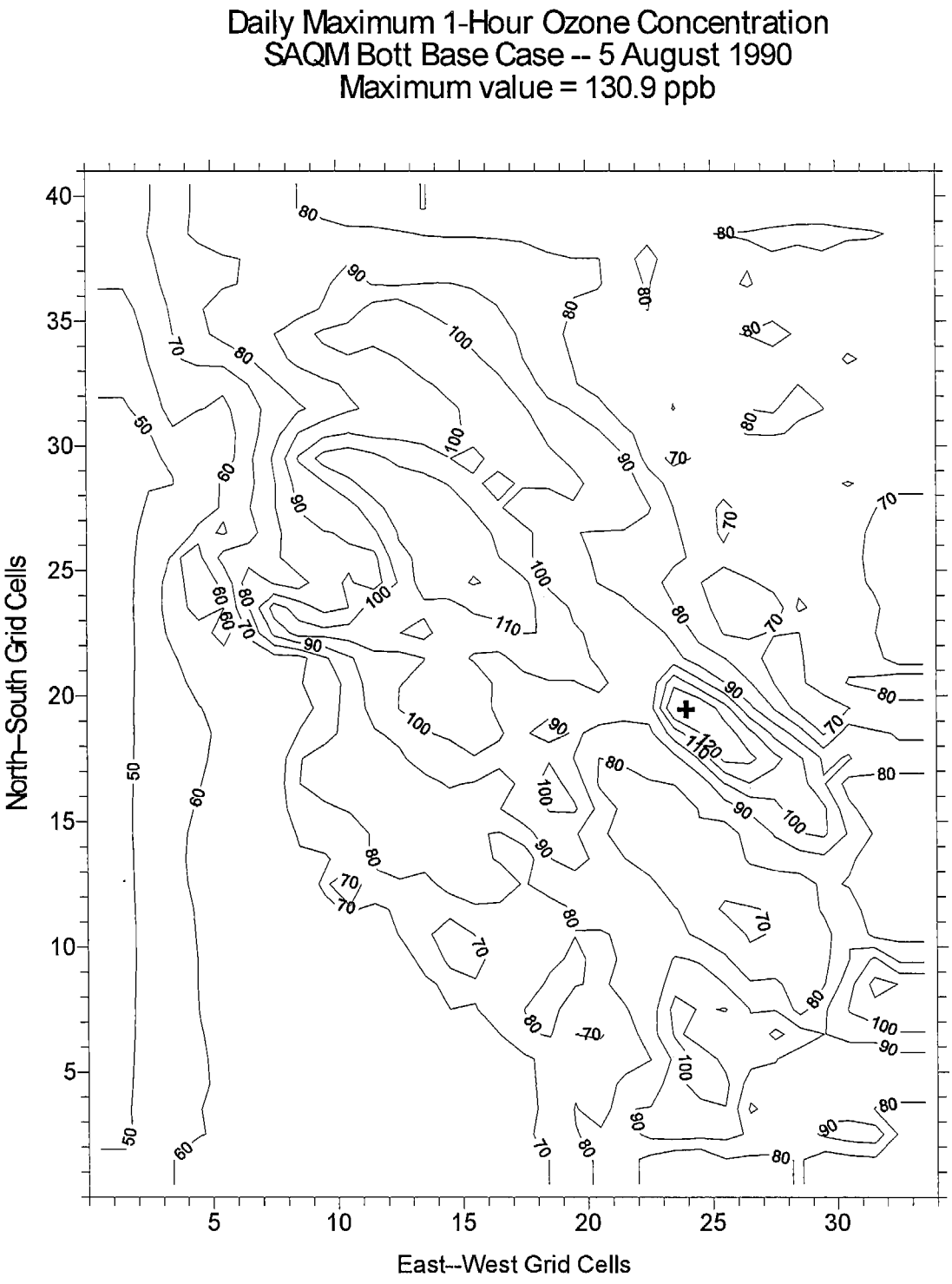

Figure 4-1a. SAQM-predicted maximum daily ozone for August 5, 1990 on the SARMAP, 12km resolution domain. This run used the Bott scheme and the Base Case diffusivity of 50 m2/s.

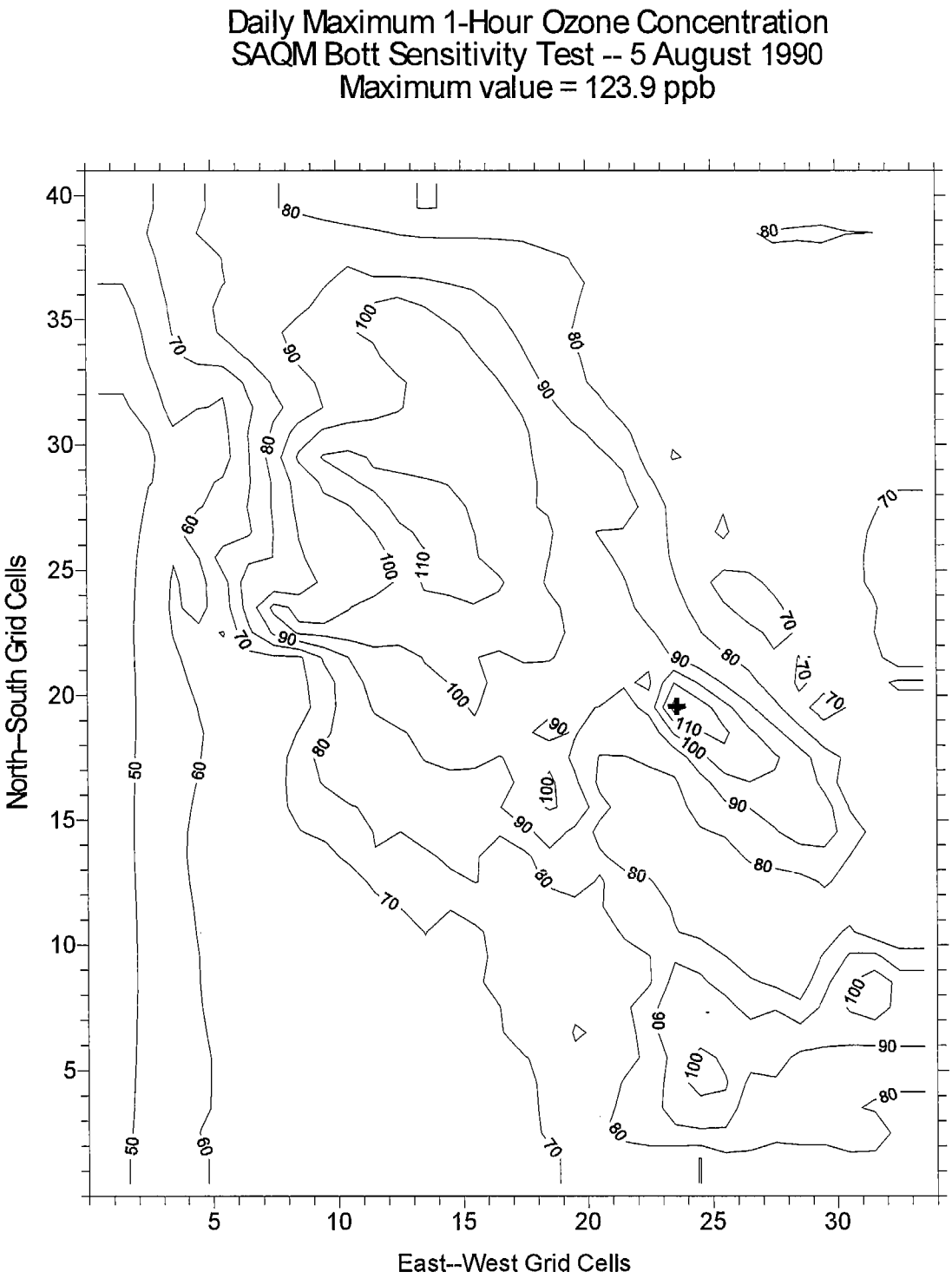

Figure 4-1b. SAQM-predicted maximum daily ozone for August 5, 1990 on the SARMAP, 12km resolution domain. This run used the Bott scheme and the simple, wind-speed proportional diffusivity designed as an enhanced diffusivity, "Sensitivity" test case.

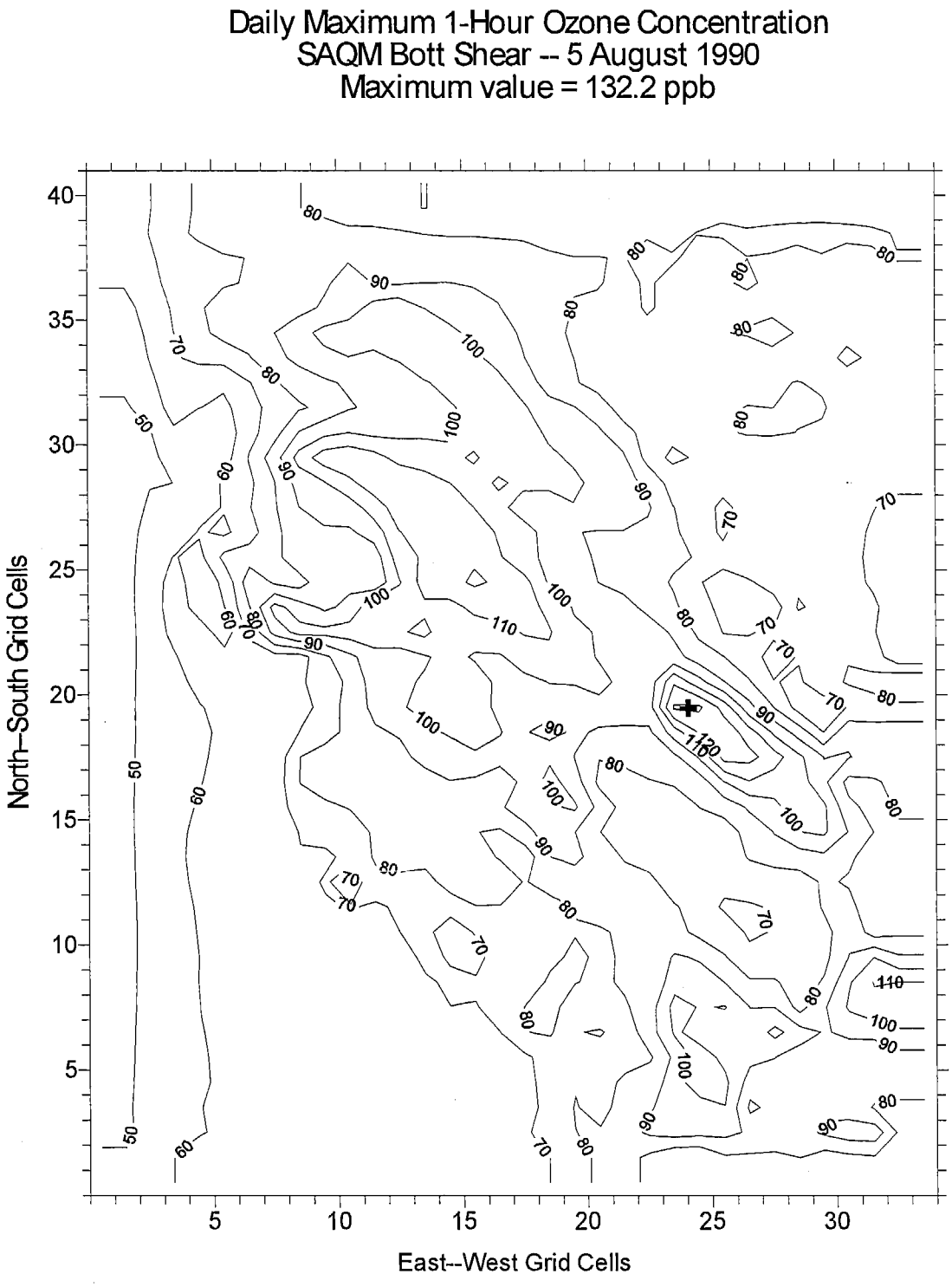

Figure 4-1c. SAQM-predicted maximum daily ozone for August 5, 1990 on the SARMAP, 12km resolution domain. This run used the Bott scheme, the original diffusivity of 50 m^2/s, and the module to correct for wind shears.

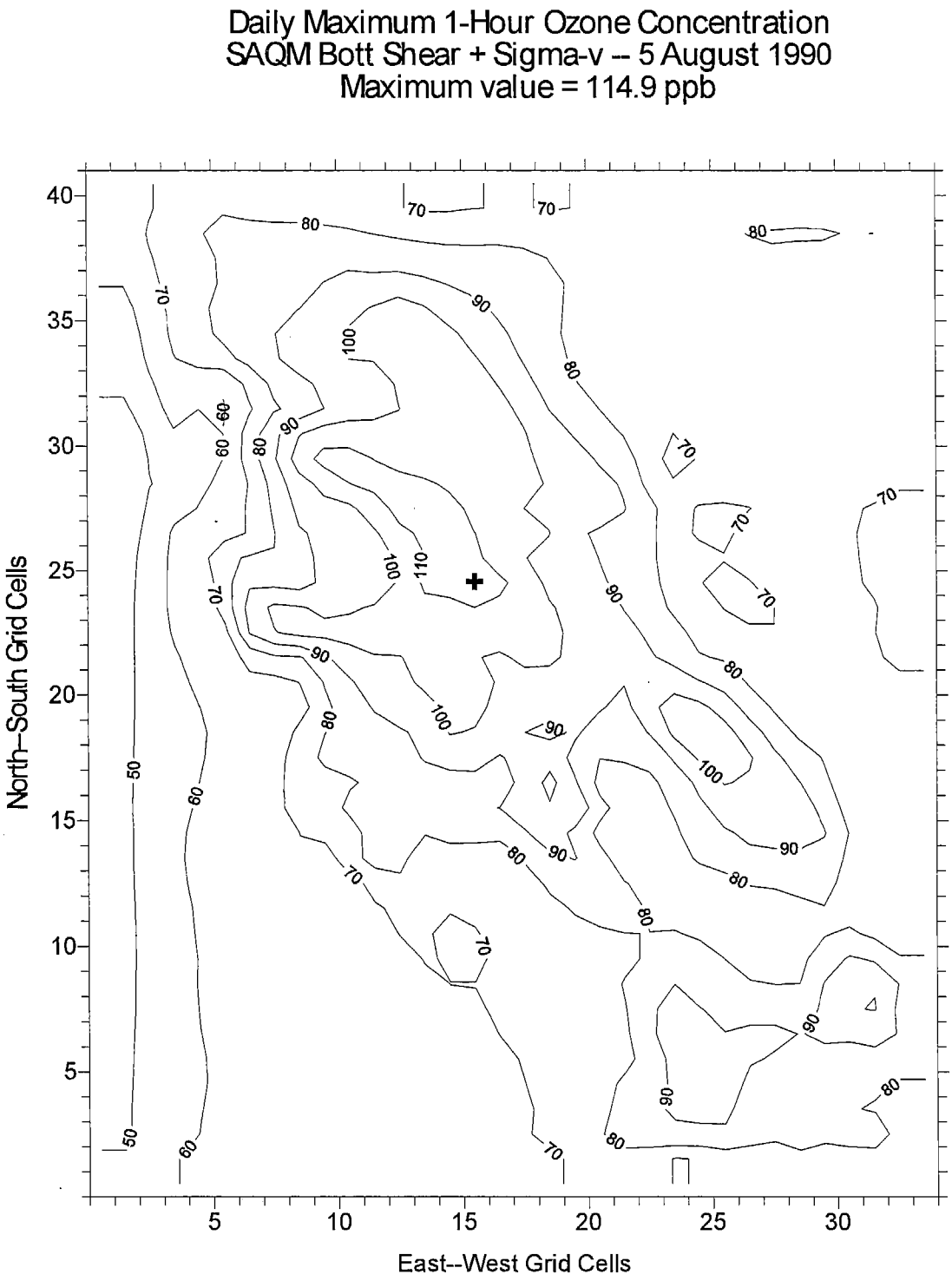

Figure 4-1d. SAQM-predicted maximum daily ozone for August 5, 1990 on the SARMAP, 12km resolution domain. This run used the Bott scheme, the module to correct for wind shears, and the module to estimate diffusivity based on modeled σ_v.

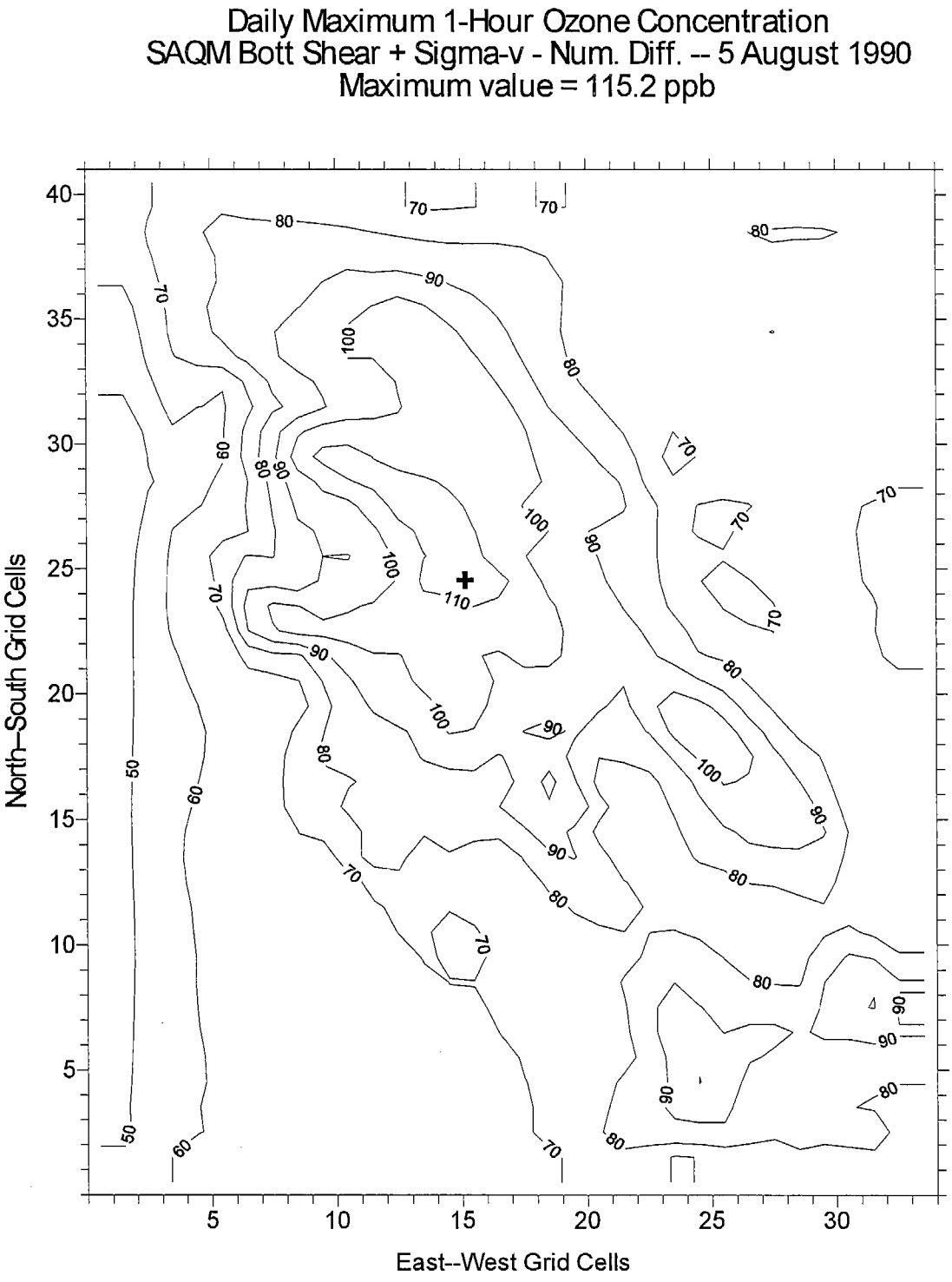

Figure 4-1e. SAQM-predicted maximum daily ozone for August 5, 1990 on the SARMAP, 12km resolution domain. This run used the Bott scheme, the module to correct for wind shears, the module to estimate diffusivity based on modeled σ_v, and minus a modeled correction for numerical diffusion.

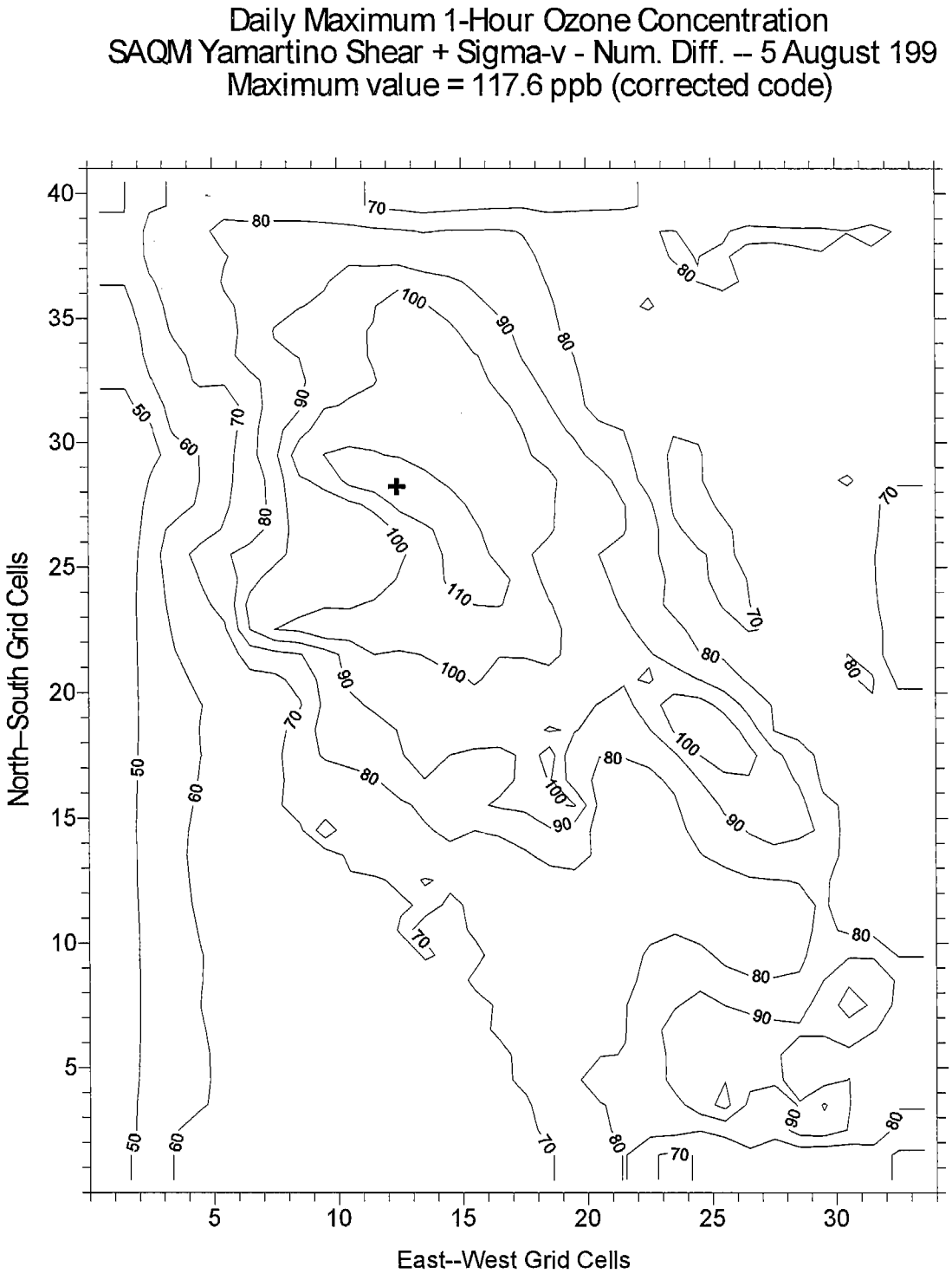

Figure 4-1f. SAQM-predicted maximum daily ozone for August 5, 1990 on the SARMAP, 12km resolution domain. This run used the Yamartino scheme, the module to correct for wind shears, the module to estimate diffusivity based on modeled σ_v, and minus a modeled correction for numerical diffusion.

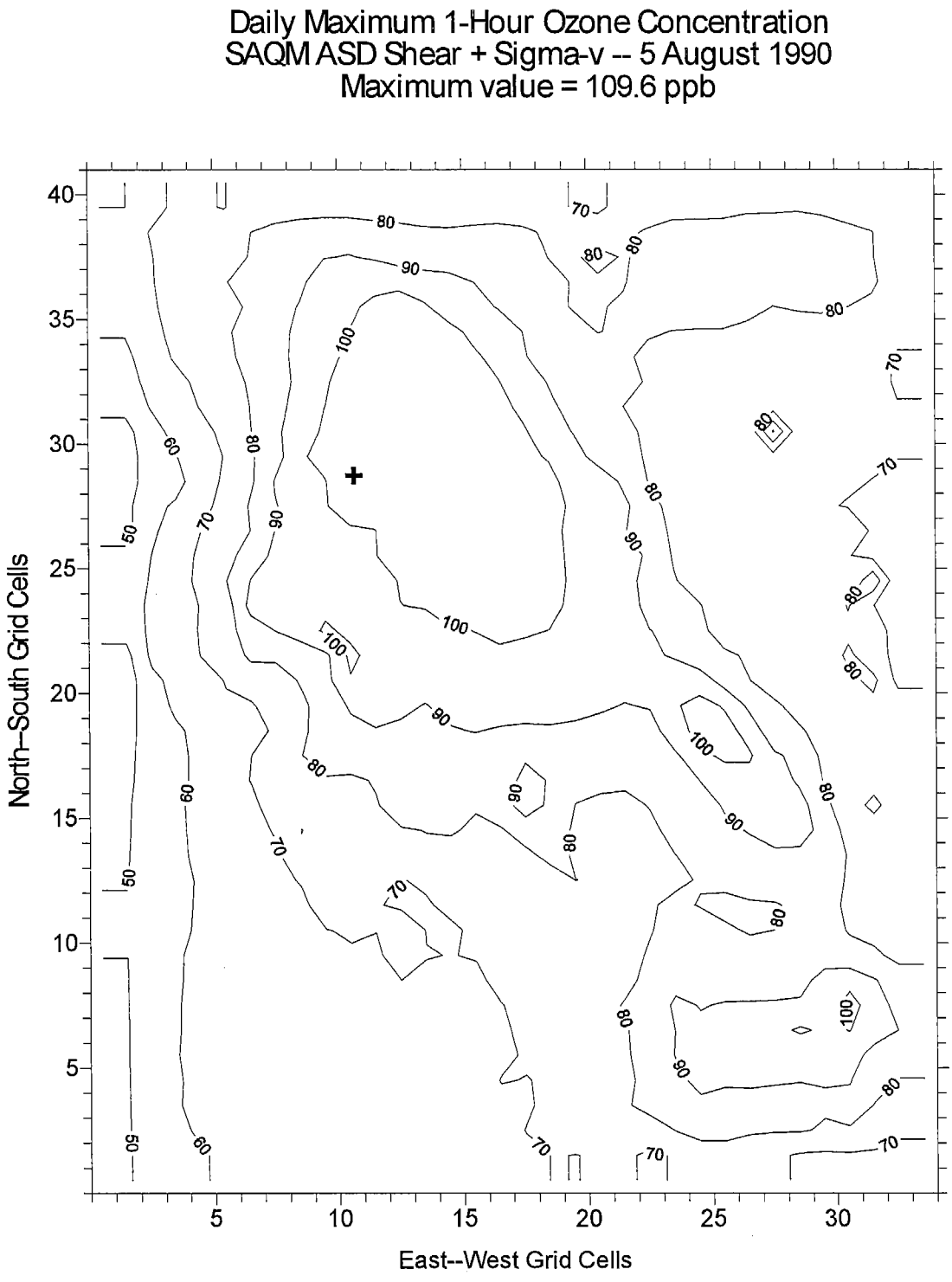

Figure 4-1g. SAQM-predicted maximum daily ozone for August 5, 1990 on the SARMAP, 12km resolution domain. This run used the ASD scheme, the module to correct for wind shears, the module to estimate diffusivity based on modeled σ_v, and a null correction for numerical diffusion.

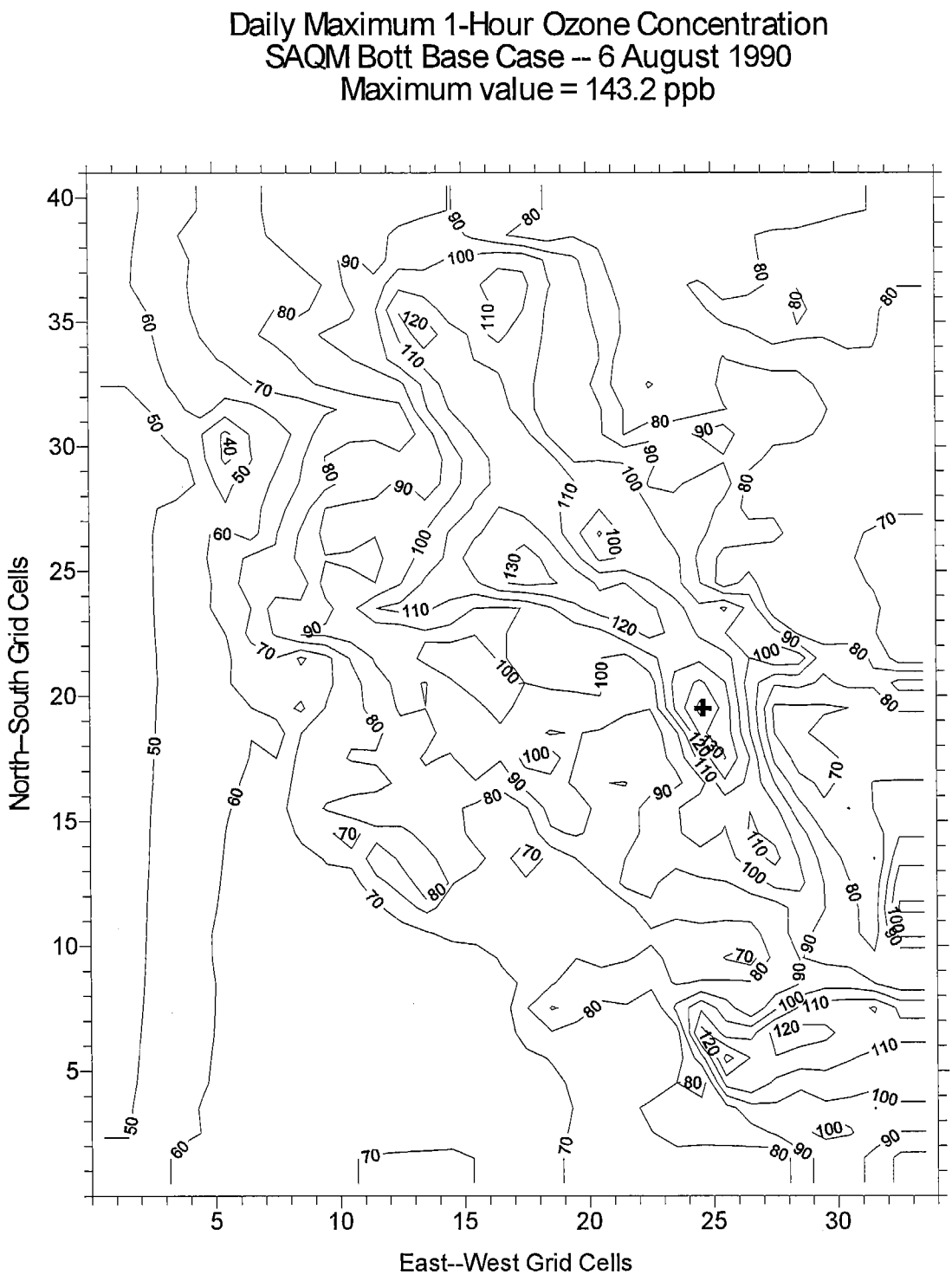

Figure 4-2a. SAQM-predicted maximum daily ozone for August 6, 1990 on the SARMAP, 12km resolution domain. This run used the Bott scheme and the Base Case diffusivity of 50 m^2/s.

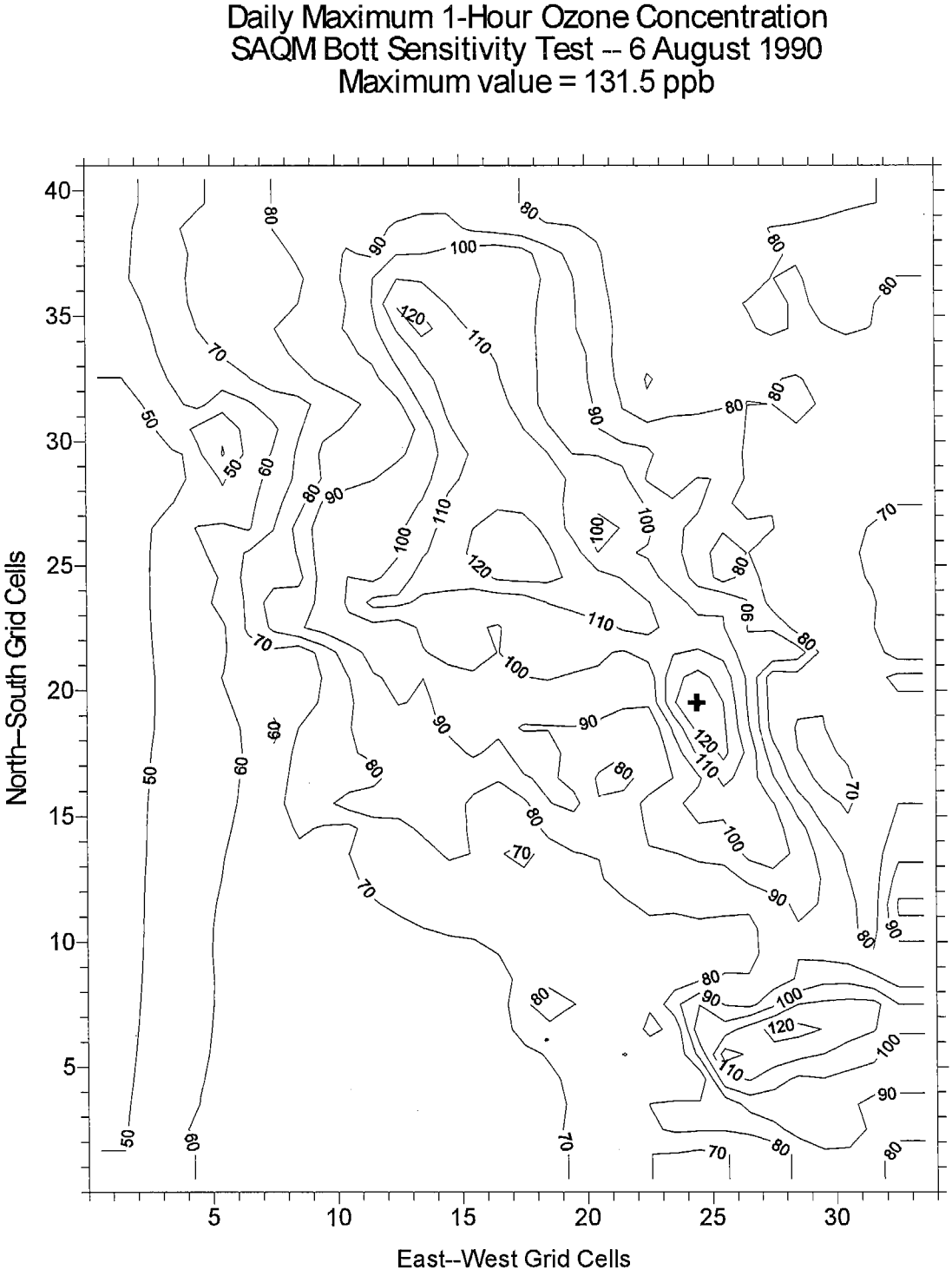

Figure 4-2b. SAQM-predicted maximum daily ozone for August 6, 1990 on the SARMAP, 12km resolution domain. This run used the Bott scheme and the simple, wind-speed proportional diffusivity designed as an enhanced diffusivity, "Sensitivity" test case.

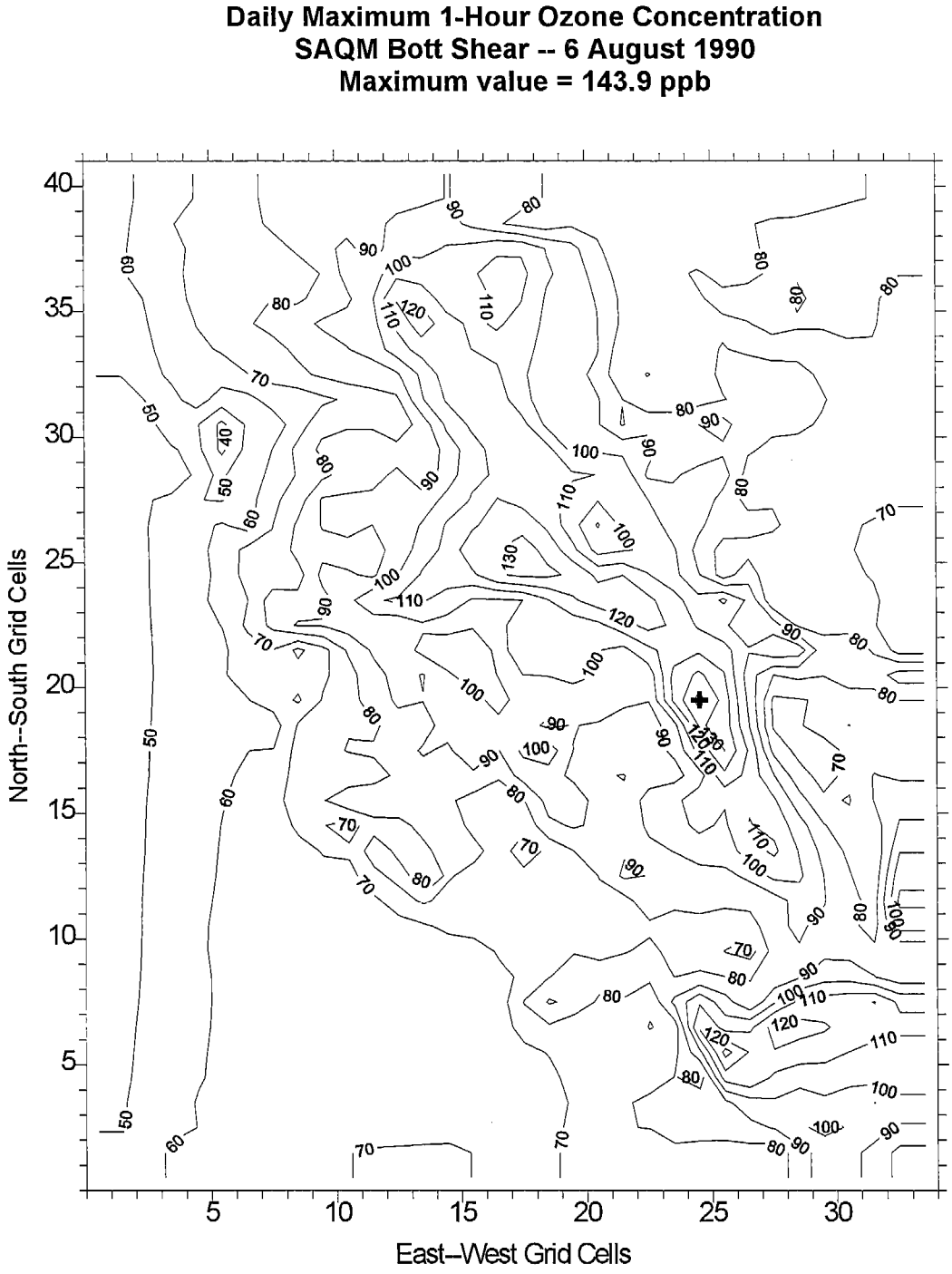

Figure 4-2c. SAQM-predicted maximum daily ozone for August 6, 1990 on the SARMAP, 12km resolution domain. This run used the Bott scheme, the original diffusivity of 50 m^2/s, and the module to correct for wind shears.

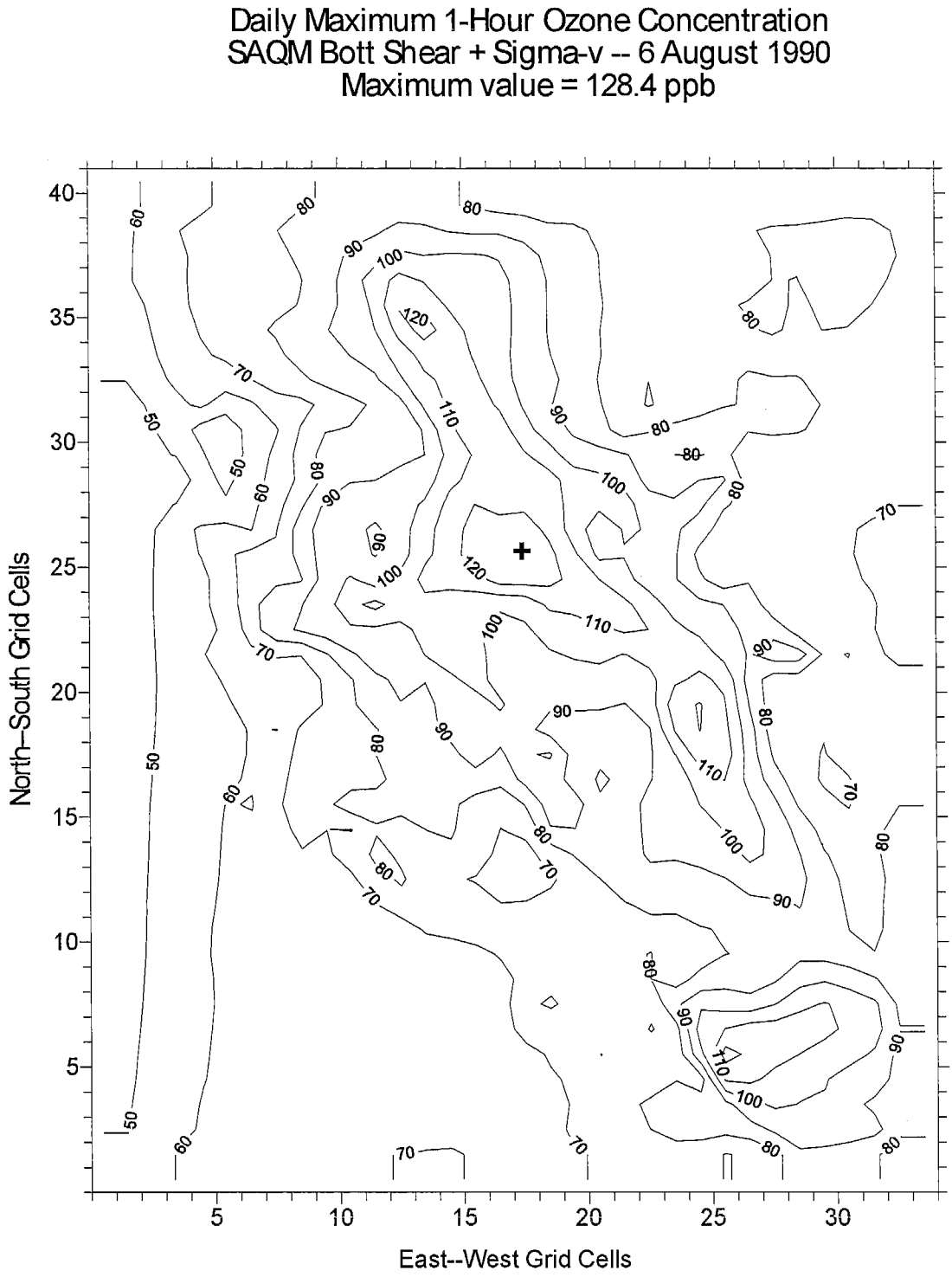

Figure 4-2d. SAQM-predicted maximum daily ozone for August 6, 1990 on the SARMAP, 12km resolution domain. This run used the Bott scheme, the module to correct for wind shears, and the module to estimate diffusivity based on modeled σ_v.

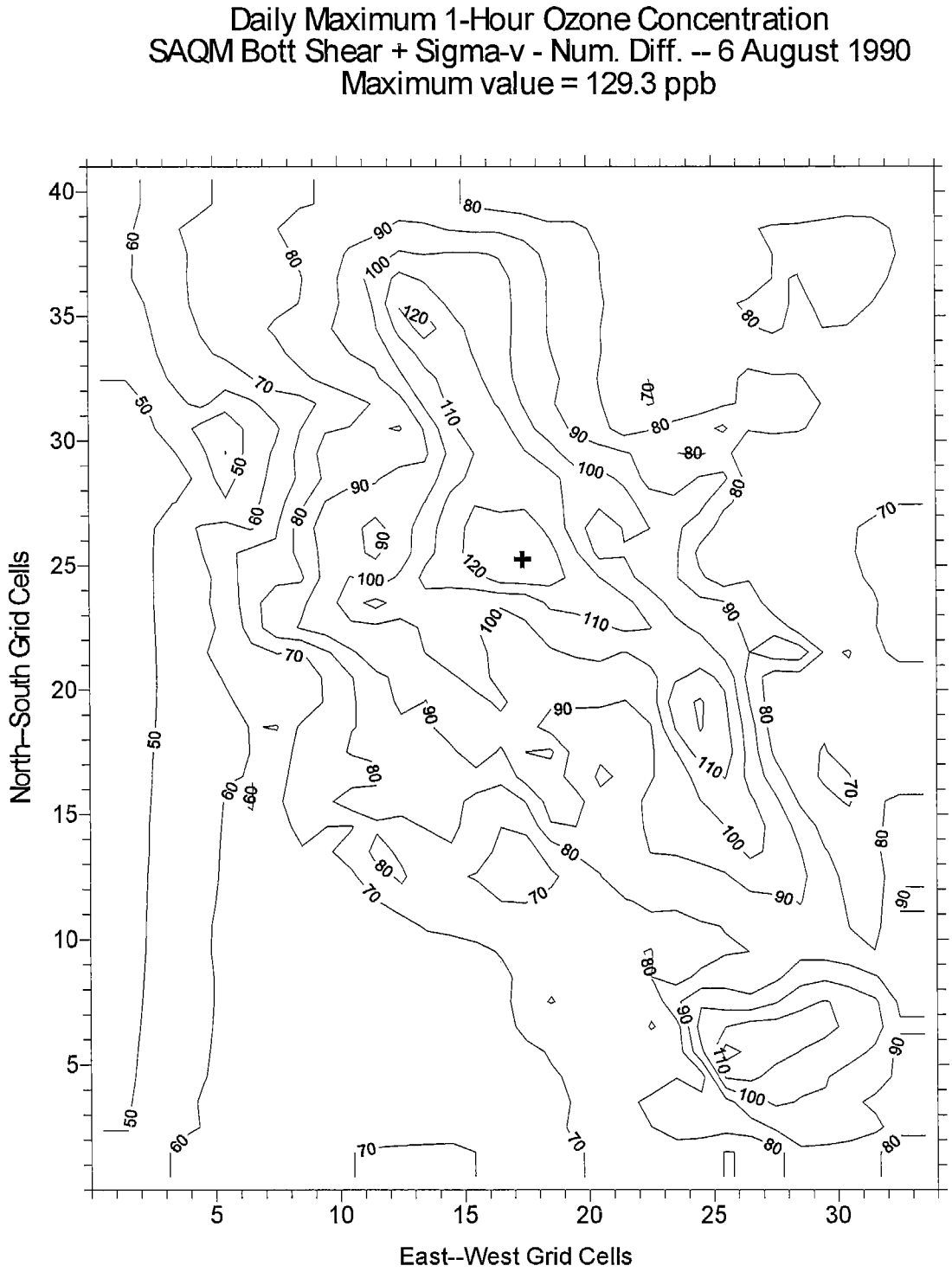

Figure 4-2e. SAQM-predicted maximum daily ozone for August 6, 1990 on the SARMAP, 12km resolution domain. This run used the Bott scheme, the module to correct for wind shears, the module to estimate diffusivity based on modeled σ_v, and minus a modeled correction for numerical diffusion.

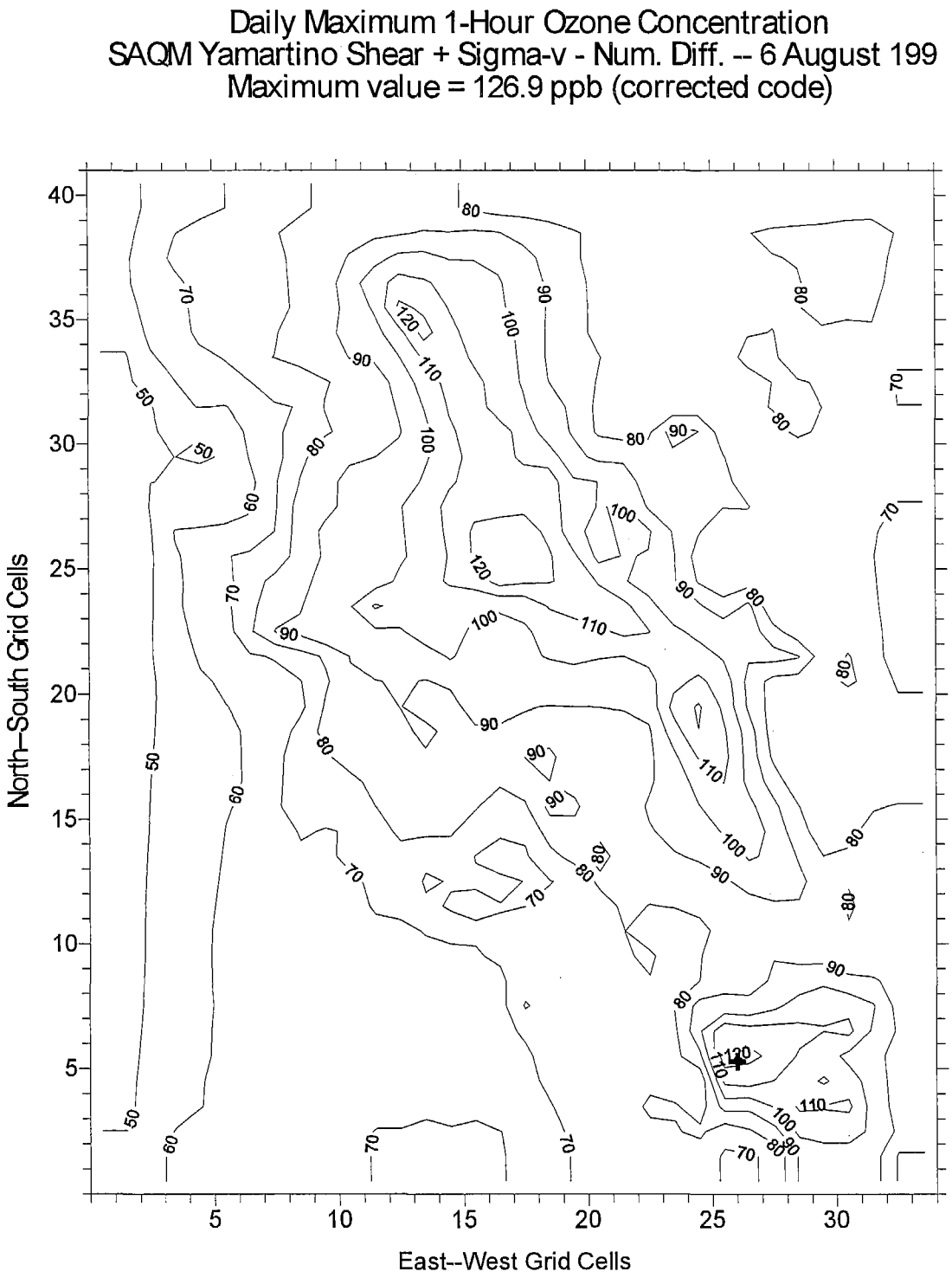

Figure 4-2f. SAQM-predicted maximum daily ozone for August 6, 1990 on the SARMAP, 12km resolution domain. This run used the Yamartino scheme, the module to correct for wind shears, the module to estimate diffusivity based on modeled σ_v, and minus a modeled correction for numerical diffusion.

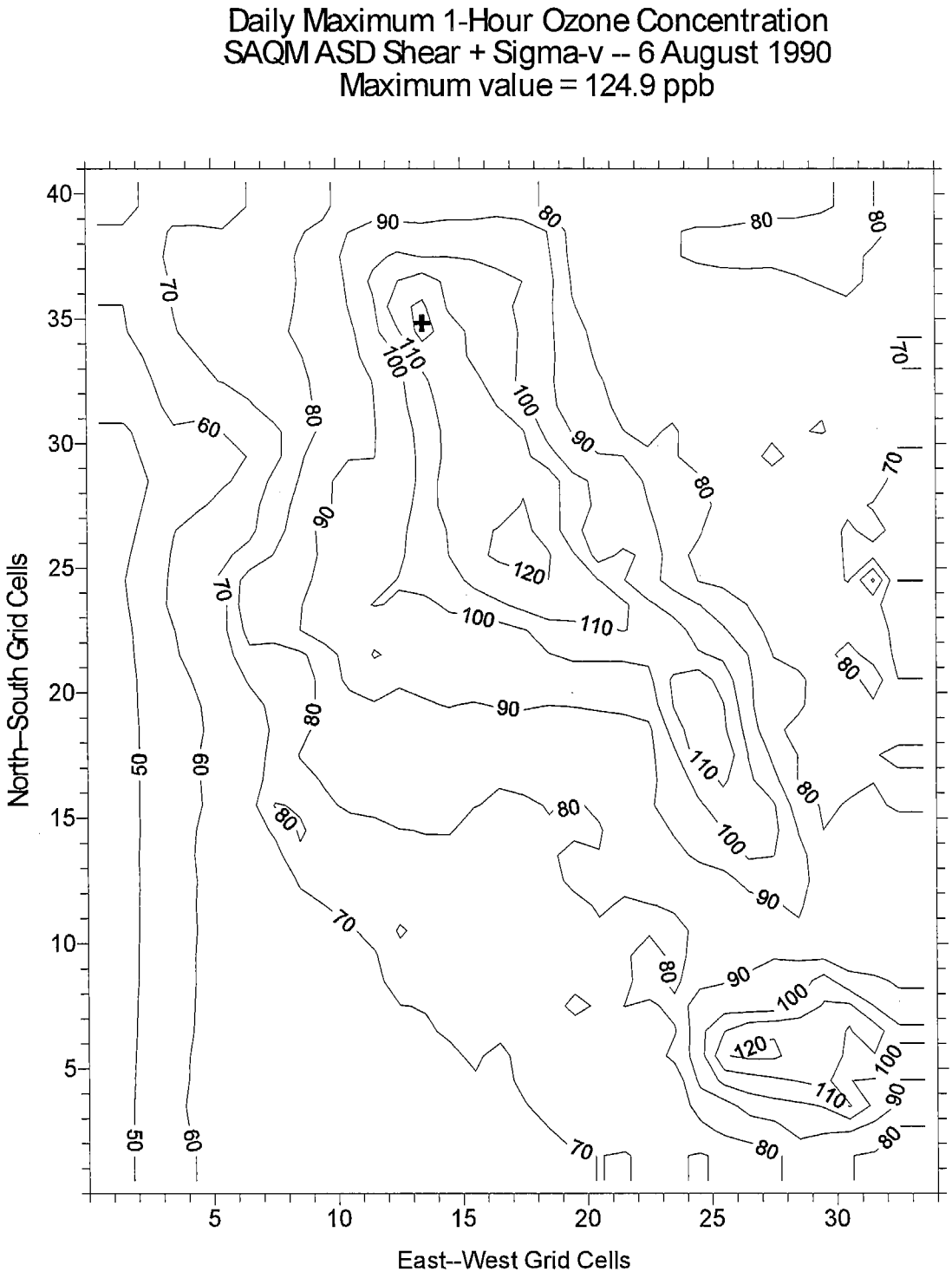

Figure 4-2g. SAQM-predicted maximum daily ozone for August 6, 1990 on the SARMAP, 12km resolution domain. This run used the ASD scheme, the module to correct for wind shears, the module to estimate diffusivity based on modeled σ_v, and a null correction for numerical diffusion.

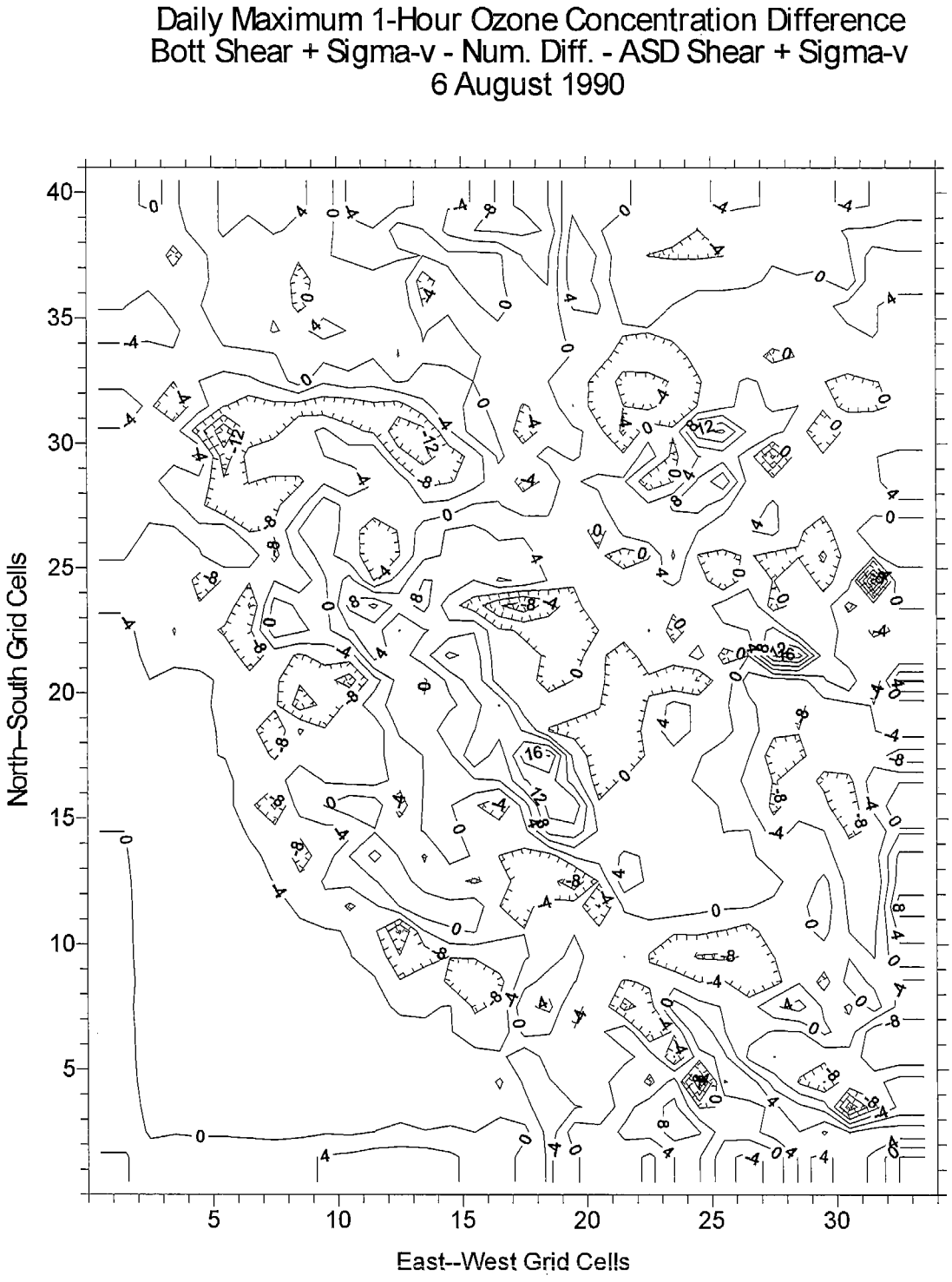

Figure 4-3. The difference field of SAQM-predicted maximum daily ozone for the Bott scheme (Fig. 4.2e) minus the ASD scheme (Fig. 4-2g) for August 6, 1990 on the SARMAP, 12km resolution domain.

5. SUMMARY AND CONCLUSIONS

A number of issues and phenomena were examined in detail as part of this study. First, the magnitude and constituent components of lateral diffusion in the atmosphere were reviewed. Given the very significant role of wind shear (e.g., shears at a particular horizontal level and turning of the wind direction with height) in the lateral diffusion process, MM-5's ability to capture wind shears was examined. Despite its similarly coarse horizontal spatial resolution, MM-5 captures 50-80% of the shear measured over separations greater than three grid cells. This suggests that the shear correction module developed for SAQM as part of this study can reasonably utilize the available MM-5 winds and achieve the appropriate advective redistribution of pollutants. MM-5's significantly higher vertical resolution assures it of capturing the important vertical wind shears, which in turn demands that the diffusivities that one utilizes in a SAQM lateral diffusivity module not "double count" this important effect. As a result, a more appropriate horizontal diffusion coefficient has been computed with the aid of a synthetic turbulence model, KSP, that can simulate lateral dispersion in an artificial atmosphere that is free of such vertical wind shear. KSP results indicated that an appropriate lateral diffusivity for 10km wide plumes in a neutral atmosphere, free of directional shear, is of order $u^* \cdot \sigma_y$, where u^* is the friction velocity and σ_y is the plume's lateral standard deviation. Extension of this concept throughout the PBL then led to a physical, non-dimensional diffusivity of $k_H = 0.2 \cdot i_y \cdot \varepsilon$, where i_y is the local turbulent intensity, σ_v/U, and ε is the local Courant number, $U \cdot \Delta t / \Delta x$. The resulting diffusivity module thus utilizes micrometeorologically-based estimates of the standard deviation of lateral velocity, σ_v, times a constant and the grid resolution, Δx, of the modeling domain.

The resulting SAQM lateral diffusivity module also incorporates the results of our investigation and subsequent parameterization of numerical diffusion. This aspect of the study revealed that the long-wave numerical diffusivities of the Bott (BOT) and Yamartino (YAM) advection schemes are comparable, larger than those of the Accurate Space Derivative (ASD) scheme, and are reasonably modeled in terms of the local Courant number, ε, and the fourth-derivative of the local concentration distribution. Numerical diffusion corrections for the Bott and Yamartino advection schemes were then implemented into the module code. The completed set of lateral transport and diffusivity modules was then smoothly and seamlessly integrated into the SAQM model simply via substitution of a number of SAQM's subroutines, and no changes to SAQM's preprocessor, input data formats, or control files were required.

Various versions of SAQM were then exercised on the August 3-6 SJVAQS ozone episode to evaluate the sensitivity of SAQM to the various components added during this study and compare the results using the three different advection schemes. These runs demonstrate that the SAQM code modifications, designed to make the treatment of diffusion in SAQM more physically realistic, were properly integrated into the current operational version of the modeling system. In addition, the resulting ozone concentrations show that improving the physical basis of the SAQM code results in a more robust simulation, that is reduced sensitivity to the advection scheme used, and has a significant effect in reducing the size and location of ozone daily maxima. SAQM peak daily ozone decreases 10-15 ppb when a plausible level of lateral diffusion is included, and the numerical-diffusion-corrected predictions of the three transport schemes generally agree to within a few ppb, though some differences can be as large as 10%.

Persisting differences between the ASD results and those of Bott and Yamartino suggest that the relatively high, short-wave, numerical diffusivities in ASD must also be compensated for before the SAQM results can be said to be truly advection scheme independent. This may be possible within the existing framework via selection of a function that declines more rapidly with increasing wavelength. Should such a simple adjustment not suffice, in-depth investigations of the emissions field relative to the concentration differences and trajectory studies may be needed to reveal more information about any transport-related aspects of the concentration differences.

6. REFERENCES

Batchelor, G.K., 1949. Diffusion in a field of homogeneous turbulence. *Austral. J. Sci. Res.* **A2**, 437-450.

Blackman, R.B. and J.W. Tukey, 1958: The Measurement of Power Spectra, New York, Dover Publications, 190 pp.

Bott, A., 1993: The monotone area-preserving flux-form advection algorithm: Reducing the time-splitting error in two dimensional flow fields. *Mon. Wea. Rev.*, **121**, 2637-2641.

Bott, A., 1992: Monotone flux limitation in the area-preserving flux-form advection algorithm. *Mon. Wea. Rev.*, **120**, 2592-2602.

Bott, A., 1989: A positive definite advection scheme obtained by nonlinear renormalization of the advection fluxes. *Mon. Wea. Rev.*, **117**, 1006-1015.

Briggs, G.A., 1973: Diffusion estimates for small emissions (Draft). Air Resources Atmospheric Turbulence and Diffusion Laboratory. ATDL No. 79. and also Internal memorandum as reported by F.A. Gifford, Jr., in Turbulent diffusion-typing schemes: a review. *Nuclear Safety*, **17**, 68-86.

Chang, J.S., K.-H. Chang, and S. Jin, 1993: Two-way and one-way nested SARMAP air quality model, Presented at the A&WMA Specialty Conference, Regional Photochemical Measurement and Modeling Studies, San Diego, CA, November 1993.

Chang, J.S. et al. (1996) The SARMAP air quality model. Final report to the California Air Resources Board.

Chock, D.P., 1991: A comparison of numerical methods for solving the advection equation-III, *Atmos. Environ.*, **25A**, 853-871.

Chock, D.P., 1985: A comparison of numerical schemes for solving the advection equation--II. *Atmos. Environ.*, **19**, 571-586.

Chock, D.P. and A.M. Dunker, 1982: A comparison of numerical methods for solving the advection equation, General Motors Report No. GMR-3603/ENV#100 and *Atmos. Environ.*, **17**, 11-24.

Crowley, W.P., 1968: Numerical advection experiments, *Mon. Wea. Rev.*, **96**, 1-11.

Dabdub, D. and J.H. Seinfeld, 1994: Numerical advective schemes used in air quality models -- Sequential and parallel implementation. *Atmos. Environ.*, **28**, 3369-3385.

DaMassa J. et al. (1996) Performance evaluation of SAQM in Central California and attainment demonstration for the August 3-6, 1990 ozone episode. Technical Report, California Air Resources Board, Sacramento, CA, 109 pp.

Dudhia, J., 1993: A non-hydrostatic version of the Penn State/NCAR Mesoscale Model: Validation tests and simulation of an Atlantic cyclone and cold front, Mon. Wea. Rev., 121, 1493-1513.

Eckman M. (1994) Re-examination of empirically derived formulas for horizontal diffusion from surface sources. Atmos. Environ. 28, 265-272.

Emde, K.V.D., 1992: Solving conservation laws with parabolic and cubic splines. *Mon. Wea. Rev.*, **120**, 482-492.

Gazdag, J., 1973: Numerical convective schemes based on accurate computation of space derivatives. *J. Comp. Phys.*, **13**, 100-113.

Gifford, F.A. (1982) Horizontal diffusion in the atmosphere: A Lagrangian-dynamical theory. Atmos. Environ. 16, 505-511.

Grell, G., J. Dudhia, and D. Stauffer, 1994: A Description of the Fifth-Generation Penn State/NCAR Mesoscale Model (MM5), NCAR/TN-398+STR, National Center for Atmospheric Research, Boulder, CO, 138pp.

Gryning S.E., Holtslag A.M., Irwin J.S. and Sivertsen B. (1987) Applied dispersion modelling based on meteorological scaling parameters. Atmos. Environ. 21, 79-89.

Hanna S.R. (1994) Random variability in mesoscale wind observations and implications for diffusion models. Proceedings of the 8th Joint Conference on Applications of Air Pollution Meteorology with A&WNA, Nashville, TN, January 23-28.

Heffter J.L. (1980) Air Resources Laboratory atmospheric transport and dispersion model (ARL-ATAD). NOAA Tech. Memo., ERL-AFL-81

Hov, O., Z. Zlatev, R. Berkowicz, A. Eliassen and L.P. Prahm, 1989: Comparison of numerical techniques for use in air pollution models with non-linear chemical reactions. *Atmos. Environ.*, **23**, 967-983.

Irwin J.S. (1983) Estimating plume dispersion — a comparison of several sigma schemes. J. Clim. appl. Met. 22, 92-114.

Janicke, L., 1995: Ausbreitungsmodell LASAT: Referenzbuch zu Version 2.51, Primelweg 8, D-88662 Überlingen, FRG. (In German)

Jin, S. and J.S. Chang, 1993: The SARMAP air quality model (SAQM), Presented at the A&WMA Specialty Conference, Regional Photochemical Measurement and Modeling Studies, San Diego, CA, November, 1993.

Long, P.E. and D.W. Pepper, 1981: An examination of some simple numerical schemes for calculating scalar advection. *J. appl. Meteor.*, **20**, 146-156.

Long, P.E. and D.W. Pepper, 1976: A comparison of six numerical schemes for calculating the advection of atmospheric pollution. Third Symposium on Atmospheric Turbulence, Diffusion, and Air Quality, Raleigh, NC, 19-22 October, 1976.

Mahrt, L, 2000. Diffusion in the Stable Boundary Layer. *Proceedings of the 11 th Joint AMS/AWMA Conference on the Applications of Air Pollution Meteorology*, Long Beach, CA, Jan. 9-14, pp 1-3.

Marchuk, G.I., 1975: Methods of Numerical Mathematics. New York, Springer-Verlag. 316 pp.

McRae, G.J., W.R. Goodin and J.H. Seinfeld, 1982: Numerical solution of the atmospheric diffusion equation for chemically reacting flows. *J. Comp. Phys.*, **45**, 1-42.

Moran, M.D., 1992. Numerical Modelling of Mesoscale Atmospheric Dispersion, Atmospheric Science Paper No. 513, Colorado State University, Fort Collins, CO, 758 pp.

Nasstrom, J.S., G Sugiyama, J.M. Leone, and D.E. Ermak, 2000. A Real-time Atmospheric Dispersion Modeling System. *Proceedings of the 11 th Joint AMS/AWMA Conference on the Applications of Air Pollution Meteorology*, Long Beach, CA, January 9-14, pp84-89.

Odman M.T., Wilkinson J.G., McNair L.A., Russell A.G., Ingram C.L. and Houyoux M.R. (1996), Horizontal advection solver uncertainty in the Urban Airshed Model. Final Report, Contract No. 93-722, California Air Resources Board, Sacramento, CA.

Odman, M.T., Xiu, A., and Byun, D.W. (1995) Evaluating advection schemes for use in the next generation of air quality modeling systems. In Regional Photochemical Measurement and Modeling Studies (edited by A.J. Ranzieri and P.A. Solomon), Vol. III, 1386-1401, Air & Waste Management Association, Pittsburgh, PA.

Odman, M.T. and A.G. Russell, 1991: Multiscale modeling of pollutant transport and chemistry. *J. Geophys. Res.*, **96**, 7363-7370.

Pack, D.H., G.J. Ferber, J.L. Heffter, K. Telegadas, J.K. Angell, W.H. Hoecker, and L. Machta, 1978. Meteorology of long-range transport. . *Atmos. Environ.*, **12**, 425-444.

Pepper, D.W., C.D. Kern and P.E. Long, 1979: Modeling the dispersion of atmospheric pollution using cubic splines and chapeau functions. *Atmos. Environ.*, **13**, 223-237.

Pielke, R.A., et al., 1992: A comprehensive meteorological modeling system - RAMS. Meteor. Atmos. Phys., 49, 69-91.

Prather M.J. (1986) Numerical advection by conservation of second-order moments. J. Geophys. Res. 91, 6671-6681.

Roache, P.J., 1976: *Computational Fluid Dynamics* (2nd edn.). Hermosa, Albuquerque, NM.

Schere, K.L., 1983: An evaluation of several numerical advection schemes. *Atmos. Environ.*, **17**, 1897-1907.

Seaman, N.L., D.R. Stauffer, and A.M. Lario-Gibbs, 1995: A multi-scale four-dimensional data assimilation system applied in the San Joaquin Valley during SARMAP. Part I: Modeling design and basic performance characteristics, J. Appl. Meteorol., 34, 1739.

Smagorinsky, J., 1963: General circulation experiments with the primitive equations: 1. The basic experiment. *Mon. Weath. Rev.*, **91**, 99-164.

Stauffer, D.R. and N.L. Seaman, 1994: Multiscale four-dimensional data assimilation, Mon. Wea. Rev., 33, 416-434.

Tanrikulu S. and Odman M.T. (1996) The effects of advection solvers on the performance of air quality models. Presented at the 5th International Conference on Atmospheric Sciences and Applications to Air Quality, Seattle, Washington, June 18-20, 1996.

Tesche T.W. et al. (1990) Improvement of procedures for evaluating photochemical models. Radian Corporation, Report to the California Air Resources Board

Tremback, C.J., J. Powell, W.R. Cotton and R.A. Pielke, 1987: The forward-in-time upstream advection scheme: Extension to high orders. *Mon. Wea. Rev.*, **115**, 540-555.

U.S. EPA, 1987: Industrial Source Complex (ISC) dispersion model user's guide -- Second edition (revised). EPA-450/4-88-002.

van Eykeren, J., Th. van Stijn and N. Praagman, 1987: A comparative investigation of numerical methods for advective processes. In *Air Pollution Modeling and Its Application VI* (edited by H. van Dop), pp. 641-652. Plenum Press, New York.

Yamartino, R.J., 2000. Refinement of Horizontal Diffusion in Photochemical Grid Models. *Proceedings of the 11 th Joint AMS/AWMA Conference on the Applications of Air Pollution Meteorology*, Long Beach, CA, January 9-14, pp226-229.

Yamartino, R.J., 1998. Improvements to Horizontal Transport in Grid Models. *Proceedings of the 23rd NATO/CCMS ITM on Air Polluting Modeling and its Application*, Varna, Bulgaria, Sept. 28 - Oct. 2.

Yamartino, R. and D. Strimaitis, 1998. Refinement and Evaluation of the Kinematic Simulation Particle Model. EARTH TECH Final Report to the German Umweltbundesamt, Sept.

Yamartino, R.J., 1993: Nonnegative, conserved scalar transport using grid-cell-centered, spectrally constrained Blackman cubics for applications on a variable-thickness mesh. *Mon. Wea. Rev.*, **121**, 753-763.

Yamartino, R.J., J.S. Scire, G.R. Carmichael and Y.S. Chang, 1992: The CALGRID mesoscale photochemical grid model--I. Model formulation. *Atmos. Environ.*, **26A**, 1493-1512.

Yamartino, R.J., J.S. Scire, S.R. Hanna, G.R. Carmichael and Y.S. Chang, 1989: CALGRID: A mesoscale photochemical grid model. Volume 1: Model formulation document, California ARB Report, Sacramento, CA.

Yamartino, R.J. and J.S. Scire, 1984: The transport and diffusion modules, Volume 3. ADOM/TADAP Model Development Program, Ontario Ministry of the Environment, Rexdale, Ontario, Canada.

Yanenko, N.N., 1971: *The Method of Fractional Steps*. Springer, New York.

Appendix A

Project-Related Papers by the Principal Investigator

1. Improvements to Horizontal Transport in Grid Models. *Proceedings of the 23rd NATO/CCMS ITM on Air Polluting Modeling and its Application*, Varna, Bulgaria, Sept. 28 - Oct. 2, 1998.

2. Refinement of Horizontal Diffusion in Photochemical Grid Models. *Proceedings of the 11 th Joint AMS/AWMA Conference on the Applications of Air Pollution Meteorology*, Long Beach, CA, January 9-14, 2000.

Prepared for the Preprints of the
Twenty-Third NATO/CCMS ITM on
Air Pollution Modeling and Its Applications
Sept. 28 - Oct. 2, 1998
Varna, Bulgaria

IMPROVEMENTS TO HORIZONTAL TRANSPORT IN GRID MODELS

R.J. Yamartino

Atmospheric Studies Group
EarthTech, Inc.
196 Baker Avenue
Concord, MA 01742 USA

INTRODUCTION

The last decade has witnessed significant improvements in the quality of advection schemes in terms of reduced amounts of numerical dispersion and diffusion. The levels of numerical diffusion are now down to the point where one has to be concerned about adding back amounts of diffusion that are appropriate to the atmospheric conditions being modeled. Determination of the appropriate horizontal diffusion coefficients that should be used in a model requires that one compute them as the total desired diffusivity minus the numerical diffusivity already accompanying the advection scheme; that is, $K_{HM} = K_{HT} - K_{HN}$. Even the numerical diffusivity, K_{HN}, known to vanish at Courant (CFL) numbers, $\varepsilon_x = u \cdot \Delta t/\Delta x$, of 0, -1, and +1 with flux formulation algorithms, and peak at CFL of +1/2 and -1/2, must first be modeled if K_{HM} is to be properly characterized as a function of CFL. It also is important to realize that the "total" diffusivity may involve a number of different processes, such as temporal wind field variations (e.g., sub-grid-scale turbulence and grid-scale wind meander) that are unresolved or dissipated by the wind field model. In addition, there are other transport errors which begin to become evident with these higher quality transport schemes; specifically, operator splitting errors and shear flow errors, which were heretofore buried by the numerical diffusion. Some of the effects of wind shear, for example, are genuinely transportive rather than diffusive, but may be lumped into the diffusivity for expediency. The mathematical characterization of these diffusivity and error terms will be detailed in the paper along with proposed corrections.

OPERATOR SPLITTING CORRECTIONS

Nearly all of the mesoscale and regional scale oxidant and acid rain models in existence today employ operator splitting (Yanenko, 1971) to solve the advection-diffusion partial differential equation (PDE) including linear and non-linear (i.e., 2nd order chemistry) source and sink terms. The primary motivation for using operator splitting is that it enables the optimal numerical methods to be employed for specific elements of the overall time-development operator. Numerous authors, including McRae et al. (1982) and Yamartino et al. (1992), discuss the validity, limitations and ramifications of invoking the symmetric operator splitting approximation, but the most important ramification from the point of view of choosing the horizontal advection scheme is that the truncation error of a model based on operator splitting plus operator reversal is second-order in time (Marchuk, 1975), even for suboperators having first-order in time truncation errors. Consequently, there is no clear motivation to use time-marching schemes in the advection operator above first-order in time and similarly no need to store or manipulate more than one time level of species concentrations.

Nevertheless, the second-order accuracy resulting from operator splitting can create some genuine problems, particularly in shear flows. These problems can be seen when advecting a uniform concentration distribution (i.e., C = 1) in a flow with net outflows $\Delta\varepsilon_x$ and $\Delta\varepsilon_y$ (i.e., expressed as the difference of cell face Courant numbers, $\varepsilon_x = u_f \Delta x/\Delta t$) in the x and y directions respectively. After both operators are applied, the mass remaining in the cell is correctly given as

$$M_r = (1 - \Delta\varepsilon_x)(1 - \Delta\varepsilon_y) , \qquad (1)$$

rather than as the incorrect result

$$M_r = (1 - \Delta\varepsilon_x - \Delta\varepsilon_y) \qquad (2)$$

given by the single 2-d operator. Given that Eq. (2) resembles more closely the operators emerging from a differential analysis, previous works have concerned themselves with the opposite problem: assuming that Eq. (2) was correct and that Eq. (1) was an approximation in need of correction. For example, this problem was outlined by Flatoy (1993) and his solution approach involved an iterative adjustment to the winds to ensure a constant mixing ratio. However, differential analysis usually ignores quantities that are of higher order in the differential, whereas a finite time step analysis shows that it is Eq. (2) which ignores the higher-order terms that Eq. (1) captures. One is convinced of this if one thinks of cutting slices of size ε_x and ε_y away from a unit square of material and asking how much material (i.e., area) is left. Even if Eq. (1) gives the correct amount of material remaining, the masses exiting the x and y faces are not in proper proportion due to the fact that the first operator took away the entire 'corner' of area, $a = \varepsilon_x \varepsilon_y$, when it should have only taken half the shared area or a/2. Given the operator order X then Y, one can show that the x Courant numbers, ε_x must be corrected by the multiplicative factor

$$(1 - \Delta\varepsilon_y/2) \ , \qquad (3a)$$

whereas the y (i.e., the 2nd operation) Courant numbers, ε_y must be corrected by the

multiplicative factor

$$(1 - \Delta\varepsilon_x/2)/[1 - \Delta\varepsilon_x(1-\Delta\varepsilon_y/2)] \ , \qquad (3b)$$

where the denominator of this factor effectively adjusts concentrations for the depleting effect of the first operator.

Clappier (1998) has recently proposed a comprehensive set of corrections to be made to advective fluxes (i.e., rather than the velocities) for 2-d and 3-d split-operator transport. His corrections completely eliminate the errors for the wind fields he has considered, and may constitute a complete solution even in very complex flow situations.

Though the perfect solution to this problem may presently be somewhat elusive, such Courant number corrections should be inserted into all operator split models subsequent to the 'last molecule' and other wind-shear specific corrections described below.

WIND SHEAR CORRECTIONS

The Along-Wind Gradient Transport Correction

Most Eulerian numerical transport schemes are routinely tested under flows (e.g., uniform, rotational) that contain no shear. Under moderate shears, Eulerian formulations have not performed as well as Lagrangian or semi-Lagrangian formulations which include shear corrections to their computation of the back trajectories from each grid point. With most (or all?) split-operator (i.e., separate 1-d operators for x and y) Eulerian advection algorithms, mixing ratio ripples will develop and grow with successive time steps for a time-independent, deformational flow field. For example, using the vortex (deformational) wind field suggested by Bott (1989), Bott's transport scheme, and a non-dimensional time step of 0.5, tests indicate that it took about 25 time steps for this ripple amplitude to reach 10% of the initial concentration and continued to grow to a maximum of about 20%. Fortunately, this problem can be substantially reduced using solutions that were originally introduced by Staniforth and Pudykiewicz (1984) for semi-Lagrangian schemes and more recently by Emde (1992) and Easter (1993). Similar corrections can now be made to Eulerian schemes.

The proposed Lagrangian corrections are basically equivalent to defining a corrected flux-face Courant number, $\varepsilon' = \varepsilon / (1.0 + \beta/2)$, where $\beta = \Delta u \cdot \Delta t/\Delta x$ and Δu is the difference in velocities between the flux face and its upwind counterpart. The basic principal of this approach was to find the point, $\varepsilon' \cdot \Delta x$, within the cell where the last molecule originated that passed through the flux face during the advection time step Δt. This correction is approximate and valid only for $\beta << 1$; however, if one integrates the expression $dt = dx / u(x)$ over the time step, Δt, assuming a linear variation of the wind in space, the exact result,

$$\varepsilon' = \varepsilon \cdot (1.0 - \exp(-\beta)) / \beta \ , \qquad (4)$$

where $\beta = \Delta u \cdot \Delta t/\Delta x$ and Δu is the difference in velocities between the flux face and its upwind

counterpart, is obtained. This correction is valid for all Courant numbers and β, though the usual stability criteria, $|\varepsilon| < 1$, and the supplementary criteria, $|\beta| < 1$, should be considered.

Tests conducted using this formulation showed that the ripple 'instability' was confined to about 1% amplitude even after 200 time steps and, thus, should no longer be considered a serious problem relative to the various other approximations associated with an Eulerian photochemical grid model. In addition, a realistic simulation involving time dependent winds and diffusion operators would act to diffuse any such ripples. It might also be mentioned that nearly all of this minor instability arises from the failure to correct effective Courant numbers at cell faces with the gradient in wind speed and is not an intrinsic limitation associated with operator splitting. The latter interpretation gained credibility because the instability is made more severe if one neglects to do operator reversal.

Flatoy (1993) attributed most of the above instability to errors intrinsically associated with operator splitting and he utilized an iterative adjustment to the winds to ensure a constant mixing ratio. We now see that two separate corrections: one for wind shear in the transport direction and one for operator splitting are required.

The Cross-wind Gradient Transport Correction

A final correction relates to advective fluxes due to distortion or stress in the horizontal wind field that are most often approximated as diffusive terms. For example, the CALGRID model (with cell dimensions $\Delta x = \Delta y$) used the moderately simple Smagorinsky (1963) formulation

$$K_S = \alpha_o^2 \, |D| \, (\Delta x)^2 \qquad (5a)$$

where $\alpha_o \approx 0.28$ and

$$|D| = \left[\left(\frac{\partial v}{\partial x} + \frac{\partial u}{\partial y} \right)^2 + \left(\frac{\partial u}{\partial x} - \frac{\partial v}{\partial y} \right)^2 \right]^{1/2}, \qquad (5b)$$

to characterize the impact of stress in the wind field.

In his review of horizontal diffusion processes and their representation, Hanna (1994) points out the problem that 'horizontal diffusion follows a linear growth rate with time for travel times out to a day or more' whereas K-theory diffusion leads to $t^{1/2}$ plume growth. Even if true for only a few hours, this fact stresses the importance of capturing as much of the wind field shear in the advective portion of the transport flux vector, F, given as

$$F = VC - K \rho \Delta (C/\rho) \; ; \qquad (6)$$

unfortunately, this cannot be done for the scales that are smaller than Δx. For these smaller scales we first consider the problem of u (i.e., x) transport through the face of a single grid cell. We then may write the local flux as either an advective flux,

$$F_a = \left[u + \left(\frac{\partial u}{\partial y}\right) y + \left(\frac{\partial u}{\partial z}\right) z \right] \left[C + \left(\frac{\partial C}{\partial y}\right) y + \left(\frac{\partial C}{\partial z}\right) z \right] \qquad (7a)$$

or as a diffusive flux,

$$F_d = \rho \left[K_{xx} \left(\frac{\partial (C/\rho)}{\partial x}\right) + K_{xy} \left(\frac{\partial (C/\rho)}{\partial y}\right) + K_{xz} \left(\frac{\partial (C/\rho)}{\partial z}\right) \right] . \qquad (7b)$$

Integrating Eqs. (6-7) over the facial area $\Delta y \cdot \Delta z$ of the cell and noting that the $u \cdot C$ term is the purely advective term already handled by our advection scheme and the term containing K_{xx} is the traditional diffusion term, the matching of terms enables one to extract expressions for the K tensor elements, such as:

$$K_{xy} = \frac{(\Delta y)^2}{12} \left[\left(\frac{\partial u}{\partial y}\right) \left(\frac{\partial C}{\partial y}\right) \right] / \left[\left(\frac{\partial C}{\partial y}\right) - \frac{C}{\rho} \left(\frac{\partial \rho}{\partial y}\right) \right] \qquad (8a)$$

and

$$K_{xz} = \frac{(\Delta z)^2}{12} \left[\left(\frac{\partial u}{\partial z}\right) \left(\frac{\partial C}{\partial z}\right) \right] / \left[\left(\frac{\partial C}{\partial z}\right) - \frac{C}{\rho} \left(\frac{\partial \rho}{\partial z}\right) \right] \qquad (8b)$$

which in the case of negligible density variation become

$$K_{xy} = \frac{(\Delta y)^2}{12} \left(\frac{\partial u}{\partial y}\right) \qquad (9a)$$

and

$$K_{xz} = \frac{(\Delta z)^2}{12} \left(\frac{\partial u}{\partial z}\right) . \qquad (9b)$$

Extension to the y flux-related tensor components K_{yx}, and K_{yz} is straightforward and the similarity between Eq(9) and Smagorinsky's Eq(5) becomes more striking when one realizes that $\alpha_o^2 = (0.28)^2 = 1/12.8$ or $\alpha_o^2 \approx 1/12$. Further, what this comparative analysis tells us is that rather than use the directionally blind K_S for wind shear related lateral 'diffusion' in both directions x and y, one may now selectively employ the direction-specific advective exchange fluxes, such as:

$$F_a = \left[u C + \left(\frac{\partial u}{\partial y}\right) \left(\frac{\partial C}{\partial y}\right) \frac{(\Delta y)^2}{12} + \left(\frac{\partial u}{\partial z}\right) \left(\frac{\partial C}{\partial z}\right) \frac{(\Delta z)^2}{12} \right] . \qquad (9c)$$

What is significant about Eq.(9c) is that the sign or direction of the latter two, x-direction, mass flow terms have no connection with the sign of the concentration x gradient, dC/dx. Such 'counter-gradient' flows are not normally equated with a diffusive process, but such is the nature

of the oft-ignored 'off-diagonal' terms of the diffusivity tensor. Du and Venkatram (1998) demonstrate the practical importance of the K_{xz} term even in the absence of a velocity gradient, $\partial u/\partial z$; thus, the right hand side of Eq.(9b) probably represents a portion of the off-diagonal K_{xz}.

OTHER WIND FIELD CORRECTIONS

Photochemical grid models are frequently driven by the output of diagnostic wind field generators. In such models, temperature, pressure and hence, density fields, are often computed by methods that are decoupled from the wind field computations. In addition, there is rarely any connection between the density fields of time step n with those of time step n+1. This means that while mass (e.g., grams of mass on the grid) might be completely conserved during and between both time step, ripples in the mixing ratio may appear in time step n+1 that were not present after time step n simply because the new density field (at step n+1) is unrelated to the densities at step n. The only way to eliminate these problems is to constrain the system to satisfy the full divergence relation,
$\nabla\cdot(\rho V) = -\partial\rho/\partial t$ as is done in prognostic meteorological models. While use of the correct conservation equation should be included as part of the meteorological model's divergence reduction procedure, corrections to achieve this could be approximated 'on the fly' within the dispersion model.

ACKNOWLEDGMENTS

This work was supported in part by a contract from the Research Division of the California Air Resources Board.

REFERENCES

Bott, A., 1993: The monotone area-preserving flux-form advection algorithm: Reducing the time-splitting error in two dimensional flow fields. *Mon. Wea. Rev.*, **121**, 2637-2641.

Bott, A., 1992: Monotone flux limitation in the area-preserving flux-form advection algorithm. *Mon. Wea. Rev.*, **120**, 2592-2602.

Bott, A., 1989: A positive definite advection scheme obtained by nonlinear renormalization of the advection fluxes. *Mon. Wea. Rev.*, **117**, 1006-1015.

Clappier, A., 1989: A correction method for use in multidimensional time-splitting advection algorithms: Applications to two- and three-dimensional transport. *Mon. Wea. Rev.*, **126**, 232-242.

Du, S. and A. Venkatram, 1998: The effect of streamwise diffusion on ground-level concentrations. *Atmos. Environ.*, **32**, 1955-1961.

Easter, R.C., 1993: Two modified versions of Bott's positive definite numerical advection scheme. *Mon. Wea. Rev.*, **126**, 232-242.

Emde, K.V.D., 1992: Solving conservation laws with parabolic and cubic splines. *Mon. Wea. Rev.*, **120**, 482-492.

Flatoy, 1993: Balanced wind in advanced advection schemes when species with long lifetimes are transported. *Atmos. Environ.*, **27A**, 1809-1819.

Hanna S.R. (1994) Random variability in mesoscale wind observations and implications for diffusion models. Proceedings of the 8th Joint Conference on Applications of Air Pollution Meteorology with A&WNA, Nashville, TN, January 23-28.

Marchuk, G.I., 1975: *Methods of Numerical Mathematics*. New York, Springer-Verlag. 316 pp.

McRae, G.J., W.R. Goodin and J.H. Seinfeld, 1982: Numerical solution of the atmospheric diffusion equation for chemically reacting flows. *J. Comp. Phys.*, **45**, 1-42.

Yamartino, R.J., J.S. Scire, G.R. Carmichael and Y.S. Chang, 1992: The CALGRID mesoscale photochemical grid model--I. Model formulation. *Atmos. Environ.*, **26A**, 1493-1512.

Yanenko, N.N., 1971: *The Method of Fractional Steps*. Springer, New York.

Prepared for the 11 th Joint AMS/AWMA Conference
on the Applications of Air Pollution Meteorology
Long Beach, CA, January 9-14, 2000

9.6 REFINEMENT OF HORIZONTAL DIFFUSION IN PHOTOCHEMICAL GRID MODELS

Robert Yamartino*
Earth Tech, Inc., 196 Baker Avenue, Concord, MA 01742 USA

1. INTRODUCTION

The last decade has witnessed significant improvements in the quality of advection schemes in terms of reduced amounts of numerical dispersion and diffusion. The levels of numerical diffusion are now down to the point where one has to be concerned about adding back amounts of diffusion that are appropriate to the atmospheric conditions being modeled. In addition, there are other transport errors which begin to become evident with these higher quality transport schemes; specifically, operator splitting errors and shear flow errors, which were heretofore buried by the numerical diffusion. The characterization of these various diffusivity and error terms must be modeled so that the "needed" horizontal diffusivity term can be added back into the modeling system as a "total" desired diffusivity minus the "numerical" diffusivity already accompanying the advection scheme. Even the numerical diffusivity, known to vanish at Courant (CFL) numbers of 0, -1, and +1 in flux formulation algorithms and peak at CFL of +1/2 and -1/2, was first modeled as a function of CFL and wavelength for several of the more popular current advection schemes.

The "total" diffusivity involves a number of diffusive processes, such as temporal wind field variations that are 'lost' by the wind field model, as well as processes, such as wind shear effects, that are genuinely transportive rather than diffusive, but may be lumped into off-diagonal diffusivity terms for expediency.

The characterization of several diffusivity terms are detailed in the paper, including:

- along-wind gradient transport corrections;
- cross-wind gradient transport corrections; and
- relative versus absolute diffusion in directionally sheared and unsheared flows.

As directional shear of the wind is already partially represented in the winds output by meteorological models, it became critical to model realistic atmospheric diffusivities in the absence of wind direction shear. This was accomplished using literature estimates and runs of the KSP synthetic turbulence model.

As a final step in this California Air Resources Board sponsored effort, the resulting diffusivity modules were added to the SAQM model and sensitivity tests performed on a multi-day SCAQS episode.

2. NUMERICAL DIFFUSION

Figure 1 shows the numerical diffusivities for several advection schemes as a function of Courant number, $u\Delta t/\Delta x$, for a wave of length $8\Delta x$. These values were determined by asking the question: what explicit diffusivity would yield the same peak concentration after two time steps -- the first with velocity +u, the second with velocity -u. This differs from the more theoretically grounded approach of Odman (1997) and forces the values to be on the same basis as expected, explicit atmospheric corrections. These dimension-less measures can yield very large diffusivities after scaling by $(\Delta x)^2/\Delta t$. For example, the fairly constant Chapeau function scheme diffusivity of 0.1 translates to a $K_{yy} \approx 4000$ m^2/s on the SAQM 12km grid assuming a one-hour time step. Such diffusivities are found to be already in the range of values expected for neutral-stability diffusion and must be 'subtracted out' in any explicit diffusivity modules.

3. WIND SHEAR CORRECTIONS

Both operator-split and non-operator split models suffer transport errors of order $(\Delta t)^2$ in shear flows. Yamartino (1998) considers some corrections for these errors, and Clappier (1998) has recently proposed a comprehensive set of corrections to be made to advective fluxes for 2-d and 3-d split-operator transport.

In this paper we consider a flux correction that is driven by wind gradients transverse to the transport direction and is, unfortunately, sensitive to the amount of smoothing performed by the

*Corresponding Author Address: Dr. R. Yamartino,
191 East Grand Ave. #206, Old Orchard Beach, ME 04064 USA
email: rjy@stanfordalumni.org or rjy@maine.rr.com

meteorological model responsible for producing the wind fields. This shear-related adjustment is often lumped into a model's mesoscale diffusivity. For example, the CALGRID model (Yamartino, et al., 1992) uses the moderately simple Smagorinsky (1963) formulation

$$K_S = \alpha_o^2 \, |D| \, (\Delta x)^2 \qquad (1a)$$

where $\alpha_o \approx 0.28$ and

$$|D| = \left[\left(\frac{\partial v}{\partial x} + \frac{\partial u}{\partial y} \right)^2 + \left(\frac{\partial u}{\partial x} - \frac{\partial v}{\partial y} \right)^2 \right]^{1/2} \qquad (1b)$$

to characterize the impact of stress in the wind field.

The review of Hanna (1994) points out the problem that horizontal diffusion follows a linear growth rate with time for travel times out to a day or more, whereas K-theory diffusion leads to $t^{1/2}$ plume growth. Even if true for only a few hours, this fact stresses the importance of capturing as much of the wind field shear in the advective portion of the transport flux vector, F, given as

$$F = VC - K \rho \nabla (C/\rho) \; ; \qquad (2)$$

unfortunately, this cannot be done for the scales that are of order Δx. For these smaller scales we first consider the problem of u (i.e., x) transport through the face of a single grid cell. We then may write the local flux as either an advective flux,

$$F_a = \left[u + \left(\frac{\partial u}{\partial y} \right) y + \left(\frac{\partial u}{\partial z} \right) z \right] \left[C + \left(\frac{\partial C}{\partial y} \right) y + \left(\frac{\partial C}{\partial z} \right) z \right] \qquad (3a)$$

or as a diffusive flux,

$$F_d = \rho \left[K_{xx} \left(\frac{\partial (C/\rho)}{\partial x} \right) + K_{xy} \left(\frac{\partial (C/\rho)}{\partial y} \right) + K_{xz} \left(\frac{\partial (C/\rho)}{\partial z} \right) \right] \qquad (3b)$$

Integrating Eqs.(2-3) over the facial area $\Delta y \Delta z$ of the cell and noting that the u·C term is the purely advective term already handled by our advection scheme and the term containing K_{xx} is the traditional diffusion term, the matching of terms enables one to extract expressions for the K tensor elements, such as:

$$K_{xy} = \frac{(\Delta y)^2}{12} \left[\left(\frac{\partial u}{\partial y} \right) \left(\frac{\partial C}{\partial y} \right) \right] \Big/ \left[\left(\frac{\partial C}{\partial y} \right) - \frac{C}{\rho} \left(\frac{\partial \rho}{\partial y} \right) \right] \qquad (4a)$$

and

$$K_{xz} = \frac{(\Delta z)^2}{12} \left[\left(\frac{\partial u}{\partial z} \right) \left(\frac{\partial C}{\partial z} \right) \right] \Big/ \left[\left(\frac{\partial C}{\partial z} \right) - \frac{C}{\rho} \left(\frac{\partial \rho}{\partial z} \right) \right] \qquad (4b)$$

which in the case of negligible density variation become

$$K_{xy} = \frac{(\Delta y)^2}{12} \left(\frac{\partial u}{\partial y} \right) \qquad (5a)$$

and

$$K_{xz} = \frac{(\Delta z)^2}{12} \left(\frac{\partial u}{\partial z} \right) \; . \qquad (5b)$$

Extension to the y flux-related tensor components K_{yx}, and K_{yz} is straightforward, and the similarity between Eq.(5) and Smagorinsky's Eq(1) becomes more striking when one realizes that $\alpha_o^2 = (0.28)^2 = 1/12.8$ or $\Upsilon_o^2 \approx 1/12$. Further, this comparative analysis tells us that rather than use the directionally blind K_S for wind shear related lateral 'diffusion' in both directions x and y, one may now selectively employ the direction-specific advective exchange fluxes, such as:

$$F_a = \left[uC + \left(\frac{\partial u}{\partial y} \right) \left(\frac{\partial C}{\partial y} \right) \frac{(\Delta y)^2}{12} + \left(\frac{\partial u}{\partial z} \right) \left(\frac{\partial C}{\partial z} \right) \frac{(\Delta z)^2}{12} \right] . \qquad (5c)$$

What is significant about Eq.(5c) is that the sign or direction of the latter two, x-direction, mass flow terms have no connection with the sign of the concentration x gradient, dC/dx. Such 'counter-gradient' flows are not normally equated with a diffusive process, but such is the nature of the oft-ignored 'off-diagonal' terms of the diffusivity tensor. Du and Venkatram (1998) show the practical importance of the K_{xz} term and the sign (-) of their correction agrees with that of Eq.(5c).

4. APPROPRIATE DIFFUSIVITIES

Unfortunately, the Eq.(5)-type adjustments to transport assume that the windfield generator actually captures the wind gradients. If instead, the meteorological model smoothes out the wind field, we must either estimate the degree of gradient loss or be forced to lump this effect into a diffusivity. An analysis of SARMAP domain, MM-5 winds at Δx = 4km., suggests that although MM-5 explains only about 50% of the observed surface wind variance, it accounts for about 60% of horizontal wind gradients for stations separated by 2-4 Δx and 80% for those in the 4-8 Δx range. Thus, rather than lumping these fluxes into a diffusivity that would result in erroneous $t^{1/2}$ plume growth, it seems preferable to use the modeled gradients, perhaps scaled up by a factor of order two, for use in Eq.(5) computations.

Assuming that wind shear effects are now accounted for, one must ask where appropriate mesoscale diffusivities are to be found. Plume growth rates measured in tracer experiments can not, of course, directly isolate the diffusive and wind shear contributions of the atmosphere; although model dependent analyses of such experiments could. An alternative approach might involve use of an LES model in a shear-free atmosphere. We have alternatively used the Kinematic Simulation Particle (KSP) model (Yamartino, et al., 2000) to simulate plume growth rates in a shear-free flow. Figure 2 shows total and relative diffusion plume sigmas for a 100m elevated, point source release. Particles were released in clusters of 10 every 20 seconds for one hour. These clusters then evolve in a steady, D stability atmosphere with $u^* \approx 0.5$ m/s. For a plume having a standard deviation of order 10 km, lateral diffusivities of order $K_{yy} \approx u^* \cdot \sigma_y \approx 5000$ m^2/s are extracted for the relative diffusion and may be appropriate for inclusion into the lateral diffusion module of the SARMAP air quality model.

5. CONCLUDING REMARKS

The low numerical diffusion accompanying modern advection schemes suggests that treatment of lateral diffusion in grid models should be refined; yet, review of the literature on horizontal diffusivities used in current mesoscale air quality grid models reveals values ranging from zero to 50,000 m^2/s.

The present approach separates out the plume growth due to wind shears and that due to diffusion. Preliminary results using the KSP model suggest a diffusivity of order $K_{yy} \approx u^* \cdot \sigma_y \approx 5000$ m^2/s. Though corrections for numerical diffusion intrinsic to SAQM's advection algorithm have yet to be implemented, initial runs using the 12km version of SAQM, altered to incorporate an added diffusivity term of $K_{yy}=1250 \cdot u$ m^2/s, yielded 10% lower peak ozone values than from a basecase run on a 5-day SARMAP episode. Thus, correct characterization of horizontal diffusivities can have significant implications for regulatory modeling.

6. ACKNOWLEDGEMENT AND DISCLAIMER

This work was supported in part by a prime contract from the Research Division of the California Air Resources Board. The statements and conclusions in this report are those of the Contractor and not necessarily those of the California Air Resources Board.

7. REFERENCES

Bott, A., 1989: A positive definite advection scheme obtained by nonlinear renormalization of the advection fluxes. *Mon. Wea. Rev.*, **117**, 1006-1015.

Clappier, A., 1989: A correction method for use in multi dimensional time-splitting advection algorithms: Applications to two- and three-dimensional transport. *Mon. Wea. Rev.*, **126**, 232-242.

Du, S. and A. Venkatram, 1998: The effect of streamwise diffusion on ground-level concentrations. *Atmos. Environ.*, **32**, 1955-1961.

Easter, R.C., 1993: Two modified versions of Bott's positive definite numerical advection scheme. *Mon. Wea. Rev.*, **126**, 232-242.

Emde, K.V.D., 1992: Solving conservation laws with parabolic and cubic splines. *Mon. Wea. Rev.*, **120**, 482-492.

Flatoy, F., 1993: Balanced wind in advanced advection schemes when species with long lifetimes are transported. *Atmos. Environ.*, **27A**, 1809-1819.

Hanna, S., 1994: Random Variability in Mesoscale Wind Observations and Implications for Diffusion Models. Eighth Joint Conf. on Applic. of Air Poll. Met. with AWMA, Nashville, Jan. 23-28, pp1-5.

Odman, M.T., 1997: A quantitative analysis of numerical diffusion introduced by advection algorithms in air quality models. *Atmos. Environ.*, **31**, 1933-1940.

Yamartino, R.J., D. Strimaitis, and A. Graff, 2000: Results of an Extensive Evaluation of the Kinematic Simulation Particle Model Using Tracer and Wind Tunnel Experiments. Paper 9.2 of this Conf.

Yamartino, R.J., 1998. Improvements to Horizontal Transport in Grid Models. *Proceedings of the 23rd NATO/CCMS ITM on Air Polluting Modeling and its Application*, Varna, Bulgaria, Sept. 28 - Oct. 2.

Yamartino, R.J., J.S. Scire, G.R. Carmichael and Y.S. Chang, 1992: The CALGRID mesoscale photochemical grid model--I. Model formulation. *Atmos. Environ.*, **26A**, 1493-1512.

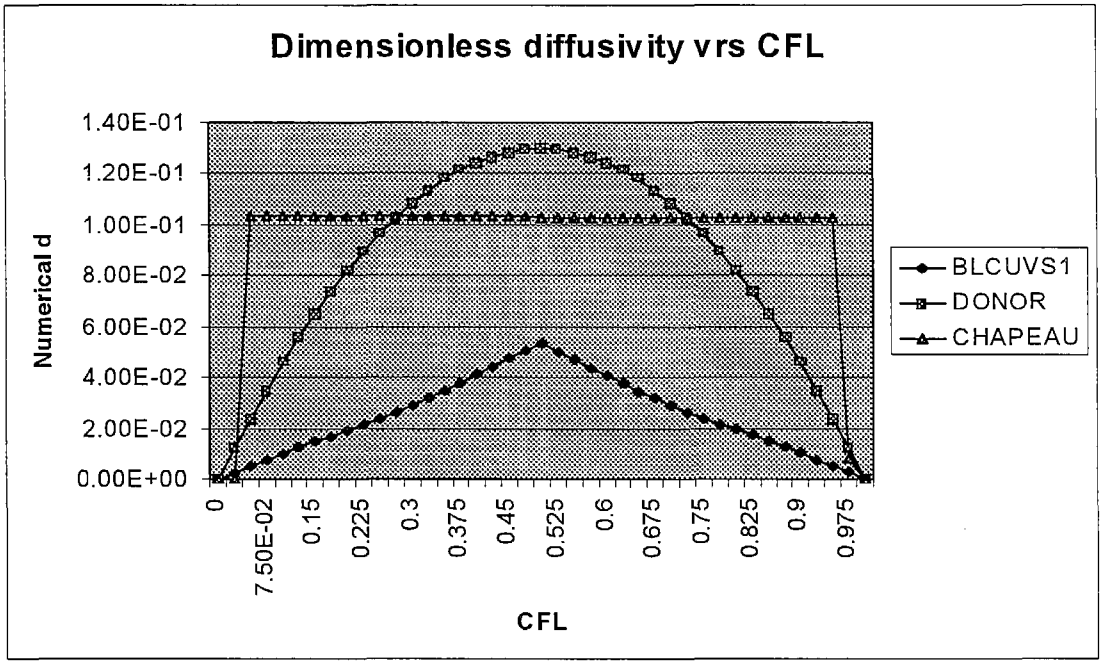

Figure 1. Dimensionless numerical diffusivities for three different advection schemes vs. Courant number for an 8□x wave. The schemes have markedly different CFL dependencies. Results are given for the donor cell, Chapeau function, and Blackman cubic methods.

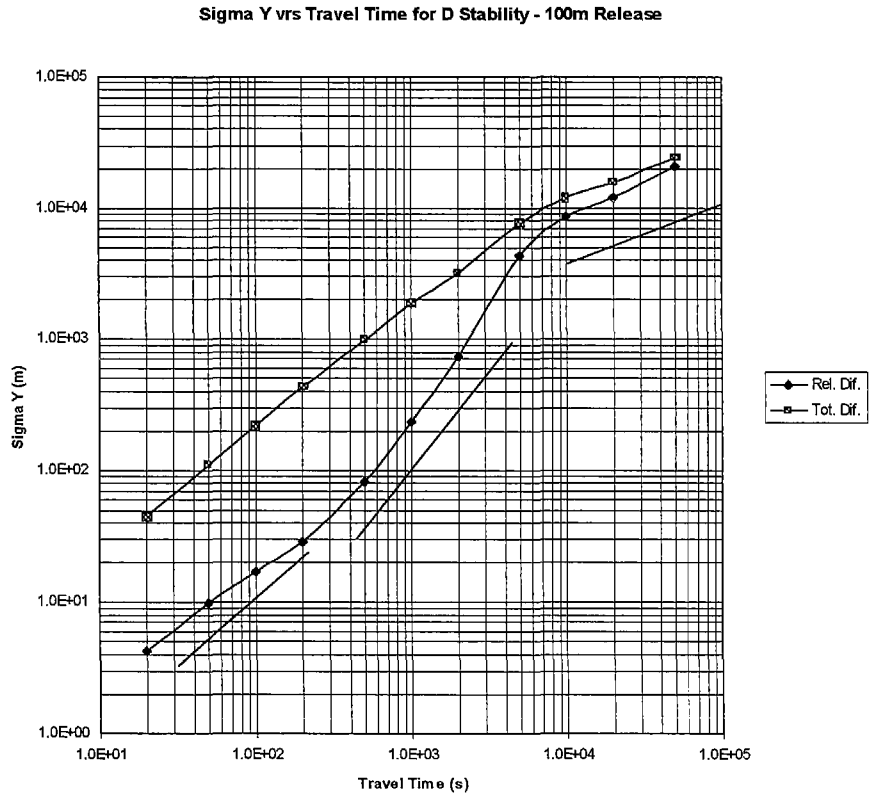

Figure 2. KSP generated total and relative diffusion estimates for 180 clusters of 10 particles released from a 100m non-buoyant source into a neutral, shear-free atmosphere. Accompanying lines indicate growth rates of t, $t^{3/2}$, and $t^{1/2}$.

Appendix B

SAQM Computer Code Modifications and Documentation

The original SARMAP Air Quality Model (SAQM) FORTRAN code is rather modular, in terms of functional units; however, many of the needed arguments within subroutines are passed through "common blocks" rather than through the call arguments to the specific subroutine. This means that modifications to SAQM can be utilized in other photochemical models provided that one is careful about the names of variables and their different usage in various models. In order to avoid confusion with existing SAQM variable and array names, the new and modified routines make use of ten (10) new 2-dimensional arrays, all contained within the new INCLUDE file, a_windg.com, and its named common block, /windgrad/ shown below:

```
common/windgrad/ epsx(imax,jmax),epsy(jmax,imax),
     1           difx(imax,jmax),dify(jmax,imax),
     2           ugrady(imax,jmax),ugradz(imax,jmax),
     3           vgradx(jmax,imax),vgradz(jmax,imax),
     4           sigw(jmax,imax),sigv(jmax,imax)
```

These arrays are specified for a specific 2-d X-Y (or Y-X) horizontal plane, and are reused as the vertical level index changes. The content of these arrays is as specified below:

VARIABLE	TYPE	DESCRIPTION
epsx(i,j)	Real*4	nondimensional X CFL (i.e., u*dt/dx) array
epsy(j,i)	Real*4	nondimensional Y CFL (i.e., v*dt/dy) array
difx(i,j)	Real*4	nondimensional X diffusivity (i.e., K*dt/dx**2) array
dify(j,i)	Real*4	nondimensional Y diffusivity (i.e., K*dt/dy**2) array
ugrady(i,j)	Real*4	nondimensional X CFL gradient in y
ugradz(i,j)	Real*4	nondimensional X CFL gradient in z
vgradz(j,i)	Real*4	nondimensional Y CFL gradient in x
vgradz(j,i)	Real*4	nondimensional Y CFL gradient in z
sigw(j,i)	Real*4	vertical velocity standard deviation (m/s)
sigv(j,i)	Real*4	horizontal velocity standard deviation (m/s)

Consistent with this approach, the pre-existing horizontal diffusivity array, eddyh, contained within the INCLUDE file, a_cmmns.com, and holding the nondimensional horizontal diffusivities defined at grid-cell centers via the SAQM subroutine, INITER.f, is no longer utilized.

As these changes are all internal to the SAQM code, and there are no changes to input or output file formats, there is no real need to update the SAQM User's Guide. Similarly, and as in the original SAQM code, the model user is not presented with run control file switches to turn diffusivity options on/off. Such desired actions would instead require code modifications (e.g., the commenting out of a line or two of code) and recompilation and/or modifications to the MAKEFILE for the SAQM executable code. All the present modified SAQM subroutines have slightly different names than in the original code, so that one can return to the original code simply by generating the executable SAQM code using the original MAKEFILE.

Figure B1 shows the affected portion of the original SAQM code. The diagram begins at the routine DRIVERN.f, which accomplishes the integration of the operator-split advection, diffusion, chemistry and other operators for the meteorological time step DT. Horizontal advection is accomplished for both X and Y directions via a single call to HADVCT.f. This routine then called the 1-d Bott advection algorithm in the original SAQM. HADVCT.f was subsequently modified by Tanrikulu and Odman (1996) to exist as three separately-named routines that made use of the Bott, ASD, and Yamartino advection algorithms, respectively. Horizontal diffusion was accomplished quite simply via a call to Subroutine HDIFF, which utilized a constant, non-dimensional diffusivity, initiated in Subroutine INITER.f and stored in the 2-d array, EDDYH, to diffuse concentrations.

Figure B2 show the result of modifications generated by this project. The modified routine, DRIVERN1.f, exhibits only the minor difference of containing separate explicit calls to the HADVCT operator for X and Y advection. More significant differences are seen in the HADVCT (i.e., existing as the separately named drivers: BOTHAD_1.f, ASDHAD_1.f, and YAMHAD_1.f for utilization of the three 1-d advection routines BOT_HN.f, ASD_HN.f, and YAM_HN2.f, respectively. The major differences in these HADVCT-like drivers include:

(a) folding the time step (DT), length scale (DX) and map factors into the definition of Courant numbers epsx(i,j) and epsy(j,i). This avoids the minor error incurred in the earlier implementations of ASD and YAM, where it was implicitly assumed that the map factor did not vary over the grid; and,

(b) computing the velocity gradients in Subroutine WINDGRAD and employing these gradients, along with the concentration gradients, to correct the Courant numbers to include these effects.

It should also be noted that the designation _HN at the end of the name for the 1-d advection routine recognizes both the modified call arguments and the fact that an algorithm-specific, numerical diffusivity function, DIFFNUM, is attached to end of each 1-d advection routine. It is also worth noting that the YAM_HN2.f routine reactivates the correct outflow boundary conditions, that had been inadvertently switched-off during its earlier implementation. Though this seems like a minor issue, the effect of the incorrect outflow boundary conditions was to hinder the flow of pollutant mass out of the grid significantly, thereby shifting the magnitude and location of the O3 maximum.

Significant code modifications are also to be found in the new horizontal diffusivity routine, HDIFF_4.f.. This routine first calls Subroutine HORVEL to compute the horizontal (and vertical) velocity variance arrays, sigv(j,i) and sigw(j,i), and then calls Subroutine HORDIF for re-computation of the Courant number arrays, epsx and epsy, followed by computation of the non-dimensional diffusivity arrays, difx and dify, based on the product of local Courant numbers and turbulent intensities, as discussed in the report. HDIFF_4.f then interrogates the advection-scheme dependent function, DIFFNUM, to compute a numerical diffusivity estimate based on Courant number and an estimate of the effective wavelength of the local concentration field. This numerical diffusivity is then subtracted from the PBL theory estimated values and used to diffuse the concentration field.

As the various modified and new FORTRAN modules and their subroutine names can create some confusion, Table B1 is included to provide a description of all relevant subroutines, their purpose, and their relationship to calling and called routines.

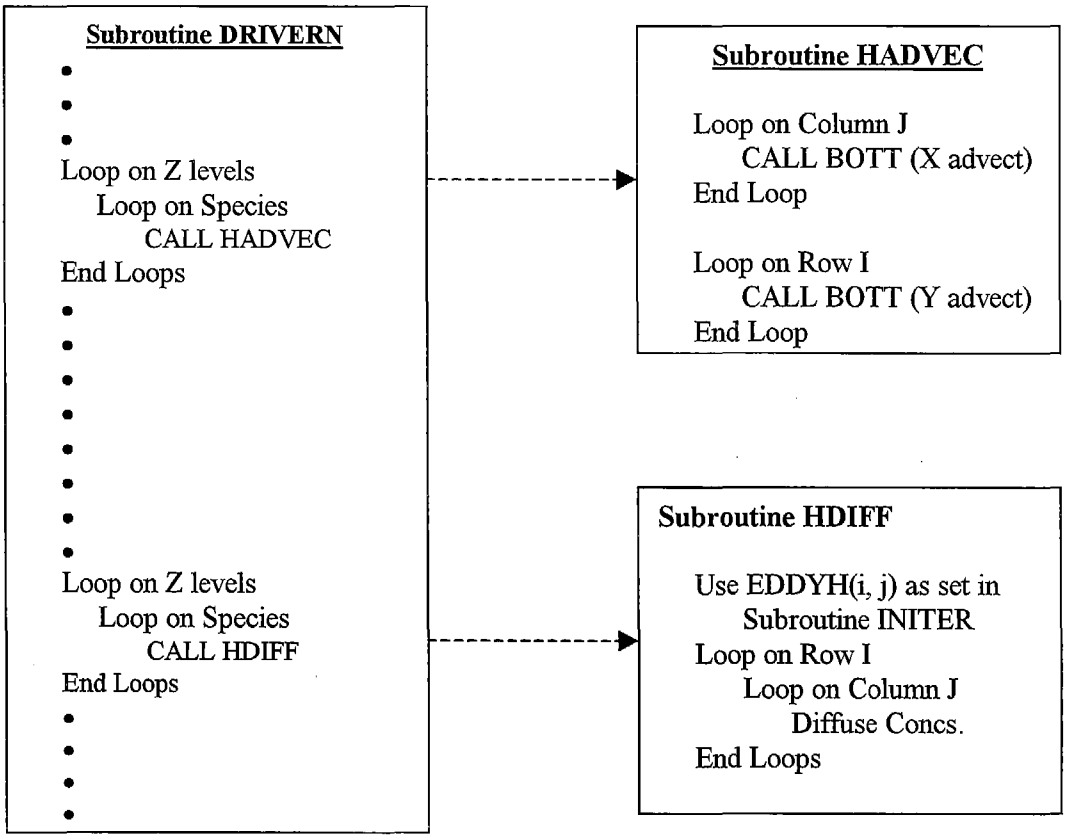

Figure B1. Flow diagram of the affected portions of the original SAQM code.

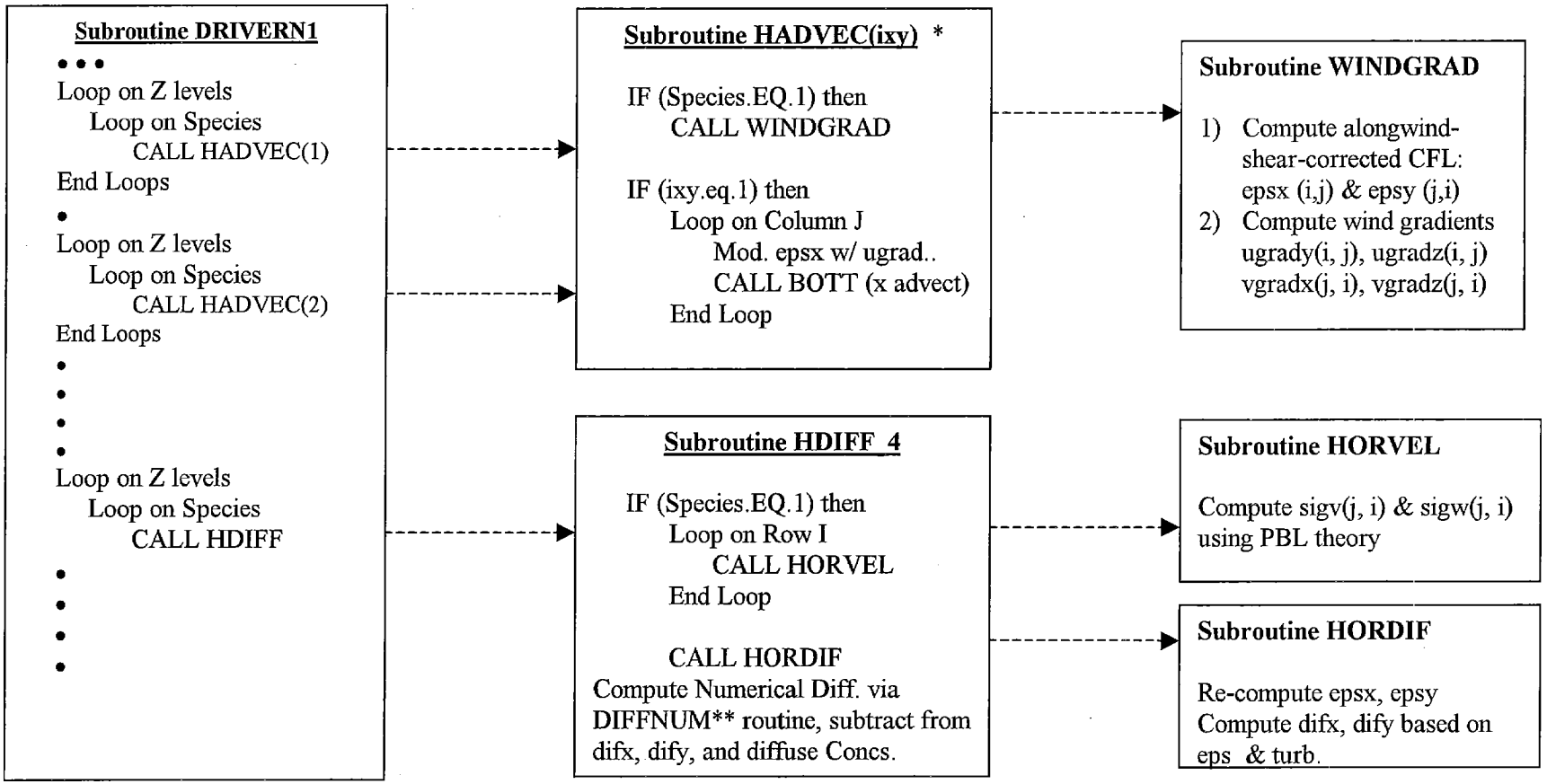

Figure B2. Flow diagram of the affected portions of the new, modified SAQM code.

* HADVEC routine exists as BOTHAD_1.f, ASDHAD_1.f, and YAMHAD_1.f for the three advection routines.

** Function DIFFNUM is defined separately for the 1-d advection routines BOT_HN.f, ASD_HN.f, and YAM_HN2.f, and attached to the end of each of these respective routines.

Table B1. Description of the new subroutines, their purpose, and their relationship to calling and called routines.

FORTRAN Module Name	Subroutine CALL Name	Status (New or Mod.)	CALLed by Subroutine	Purpose of Subroutine	This Subroutine CALLs
drivern1.f	drivern	modified	saqm2c saqmgraf	Integrates all operators one meteorological time step, DT	hadvec hdiff (w/ 4 args) and others
1) bothad_1.f 2) asdhad_1.f or 3) yamhad_1.f	hadvec	modified	drivern	Performs 2-d advection via repeated calls to 1-d advection algorithm.	windgrad and 1) bot_hn 2) asd_hn or 3) yam_hn2
1) bot_hn.f 2) asd_hn.f or 3) yam_hn2.f	1) bott_h 2) asd_h. or 3) yamartino_h	modified	hadvec	Performs 1-d advection. Now has Function Diffnum attached to end of each routine.	None (but asd_h has many calls)
windgrad.f	windgrad	new	hadvec	Computes non-dim.Courant no. and wind gradient arrays.	None
hdiff_4.f	hdiff.f	modified w/ 4 call args	drivern	Performs 2-d horizontal diffusion of species L and vertical level K	horvel hordif diffnum
horvel_3.f	horvel	new	hdiff	Compute time interp. micromet. for sigma v and sigma w calc.	sigwv
sigwv.f	sigwv	new	horvel	Computes sigma v and sigma w using PBL theory	None
hordif_3.f	hordif	new	hdiff	Re-computes non-dim.Courant no. and eddy diffusivity arrays.	None
Part of: 1) bot_hn.f 2) asd_hn.f and 3) yam_hn2.f	diffnum	new	hdiff	Computes Courant no. dependence of numerical for the specific advection scheme.	None